



3D printing for preoperative planning and surgical training: a review

Anurup Ganguli^{1,2} · Gelson J. Pagan-Diaz^{1,2} · Lauren Grant^{1,2} · Caroline Cvetkovic^{1,2,3} · Mathew Bramlet^{4,5} · John Vozenilek^{1,4,5,6} · Thenkurussi Kesavadas^{5,6} · Rashid Bashir^{1,2,7,8}

© Springer Science+Business Media, LLC, part of Springer Nature 2018

Abstract

Surgeons typically rely on their past training and experiences as well as visual aids from medical imaging techniques such as magnetic resonance imaging (MRI) or computed tomography (CT) for the planning of surgical processes. Often, due to the anatomical complexity of the surgery site, two dimensional or virtual images are not sufficient to successfully convey the structural details. For such scenarios, a 3D printed model of the patient's anatomy enables personalized preoperative planning. This paper reviews critical aspects of 3D printing for preoperative planning and surgical training, starting with an overview of the process-flow and 3D printing techniques, followed by their applications spanning across multiple organ systems in the human body. State of the art in these technologies are described along with a discussion of current limitations and future opportunities.

Keywords Rapid prototyping · Organ models · Surgical training · Preoperative planning · 3D printing

1 Introduction

Surgeons have always faced the challenging task of carrying out surgeries on complex anatomical structures of the human body. With advances in medical imaging, tools such as multi-detector computed tomography (MDCT) and magnetic resonance imaging (MRI) have made radiological diagnosis less invasive and more informative. These tools provide high resolution two-dimensional images, but are limited in their ability to accurately depict complex 3D structures. Virtual 3D reconstruction methods, such as volume

or surface rendering, offer a better understanding of structural complexity by allowing for rotation or sectioning of layers of the virtual 3D model. This ability has proven useful for the visualization of complex structures, such as congenital heart defects and aneurysms (Ou et al. 2007; Spevak et al. 2008; Kellenberger et al. 2007). However, differences between real anatomical structures and the interpretation of virtual 3D images still remain (Shiraishi et al. 2010). As a result, the success of surgical operations relies heavily on the surgeon's previous training and past experiences. To address the limitations in virtual image analysis, 3D printing is now being used to create physical models of patient anatomies for surgical simulation and preoperative planning.

Surgical simulations allow surgeons to learn new techniques or prepare for specific operations without the use of patients, cadavers, or animal models. Through physical recreation of a patient's organs or tissues, a realistic surgical procedure can be simulated. With recent advancements in the field of 3D printing, MRI or CT images can now be used to fabricate 3D anatomical models. 3D printing is a process by which 3D digital (CAD) models are converted into physical models through a layer-by-layer fabrication process. Patient-specific printed models of the anatomical region in need of surgical repair can provide the surgeon with a better visualization of the defected tissue, thus helping him to prepare for the surgery. These models can also be used to train new surgeons, given the short supply of donated human tissues and organs. A number of advantages of 3D printed models have been noted, such as better tactile understanding of an anatomy, rehearsal of the exact surgical route, implant and prosthesis

✉ Rashid Bashir
rbashir@illinois.edu

¹ Department of Bioengineering, University of Illinois at Urbana-Champaign, Urbana, IL, USA

² Micro and Nanotechnology Laboratory, University of Illinois at Urbana-Champaign, Urbana, IL, USA

³ Center for Neuroregeneration, Houston Methodist Research Institute, Houston, TX, USA

⁴ OSF Saint Francis Medical Center, University of Illinois College of Medicine at Peoria, Urbana, IL, USA

⁵ Jump Trading Simulation & Education Center, Peoria, IL, USA

⁶ Healthcare Engineering Systems Center, College of Engineering, University of Illinois at Urbana-Champaign, Urbana, IL, USA

⁷ Department of Industrial and Enterprise Systems Engineering, University of Illinois at Urbana-Champaign, Urbana, IL, USA

⁸ Carle Illinois College of Medicine, Urbana, IL, USA

planning and tailoring, easy intraoperative access for surgical guidance, and better communication between surgeon and patient (Müller et al. 2003; Kalejs and von Segesser 2009).

Given the growing interest in 3D printing for surgical simulation over the past decade, we feel there is a need for a comprehensive, systematic review of the subject. This review aims to summarize the use of 3D printing for surgical simulation in a variety of clinical areas, as well as the developed techniques to optimize the implementation of rapid prototyping to such areas. Beyond summarizing techniques, this review also aims to identify potential shortcomings in current surgical applications of 3D printing, so that future researchers can streamline their efforts towards these goals.

2 3D printing technique overview

3D printing can be broadly described as an additive fabrication process by which free-form 3D structures are formed in a layer-by-layer fashion from 3D computer models. The fabrication of physical 3D models from anatomical imaging data (MRI/CT) can be described as a 3-step process: (1) image acquisition, (2) image processing, and (3) 3D printing (Fig. 1).

The accuracy of the 3D printed object depends on the accuracy of the acquired image. Different imaging modalities used include MRI, MDCT, cone beam computed tomography (CBCT), positron emission tomography (PET), and ultrasonography (US) among others. MDCT is the most widely used modality owing to the ease of post-processing its data. Furthermore, images can be acquired with a spatial resolution of 400–600 microns, showing how MDCT offers a 3D dataset with better resolution, but can still result in procedural failure owing to the complex morphology (Rengier et al. 2010). The final images are saved in DICOM (digital imaging and communications in medicine) format.

Several software packages, such as Mimics (Materialise NV, USA) and MeVislab (Mevismedical Solutions, Germany), have been used for the post processing of images.

This software segments the images to produce a final STL file. Segmentation is the process of isolating an area of interest in the data files, where the dataset is a series of DICOM images which when stacked together form the complete structure. Advanced image processing algorithms have also been proposed for special cases like non-enhanced or low resolution images (Frakes et al. 2005). Triangular meshing is usually performed on the contours of segmented region of interest (Hahn et al. 2004). This data can be further processed using various CAD software for modification of geometry or mesh optimization. The final modified data is converted to STL format, which can then be sent to a 3D printer for fabrication.

The 3D printing machine reads data from a CAD file and adds successive layers of material, thus building the model from a series of cross-sections. Compared to alternative fabrication tools such as CNC machining, which consists of CAD-guided material removal, 3D printing is more appealing due to its geometric flexibility, lower fabrication time, lower cost and minimal technical expertise requirement. Its geometric flexibility is the main reason that 3D printing is best suited for the fabrication of complex anatomical structures. The downtime for 3D printing (a few hours) is usually lower than that for contemporary techniques (several hours to days) but actual fabrication time depends on the particular 3D printing method, as well as the complexity of the structure.

The STL file obtained from the DICOM images of the part of interest is sent to a 3D printer and the final 3D part is obtained as the output. This technique truly allows medical practitioners to employ “patient specific” surgical planning and problem understanding. Figure 1 describes this process of file preparation for the 3D printing of an anatomical model.

A common approach for converting this computational data into 3D solid models is rapid prototyping (Ngan et al. 2006; Sodian et al. 2007). Rapid prototyping is a method for 3D model fabrication from computer-generated virtual 3D surface models, usually derived from CT or MRI imaging data set. The virtual model is first broken down into thin slices or layers. A rapid prototyping machine then builds the solid

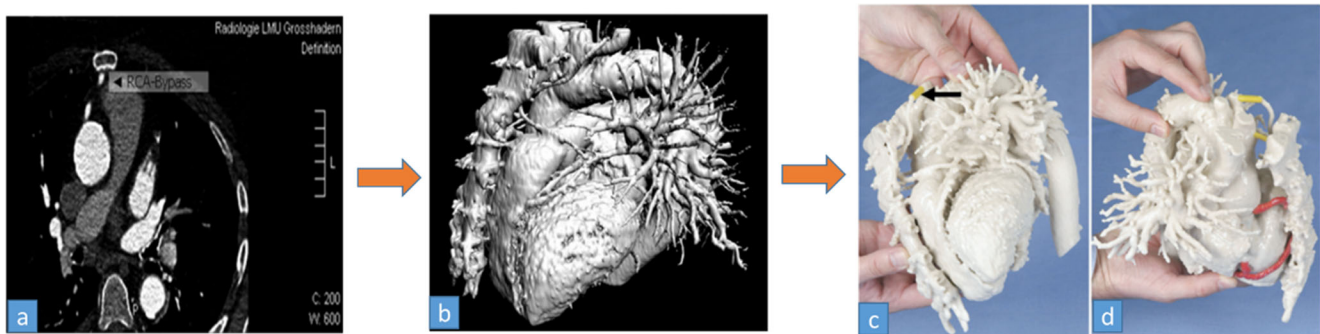


Fig. 1 Process flowchart for 3D printing models for clinical simulations. **a** Step1: *CT scan* of a patient with a patent left anterior descending artery and right coronary artery bypass close to sternum (arrow) **(b)** Step2: *Image processing*- 3D segmentation of the CT data **(c)** Step 3: *3D*

printing- SLA model of the patient's cerebrovascular anatomy (Sodian et al. 2008b). (Copyright © 2008 The Society of Thoracic Surgeons. Published by Elsevier Inc.)

model layer upon layer, resulting in a physical replica of the virtual model. Rapid prototyping encompasses several different techniques each with its own benefits and drawbacks (Fig. 2) (Park et al. 2016). Stereolithography (SLA) is one of the most common techniques, and uses an ultraviolet laser to polymerize a photo-curable resin (Winder and Bibb 2005). Fused deposition modelling (FDM) is similar to SLA with the main difference being that the layers are formed by the extrusion of small beads of fused thermoplastic material from a fine tip (Kruth 1991). Selective laser sintering (SLS) uses an infrared laser to cure thermoplastic powder (Berry et al. 1997). Laminated object manufacturing is yet another technique, which uses layers of paper or plastic cut by a laser and bonded by a heating process (Mueller and Kochan 1999).

3 3D printing technique development by surgery area

3.1 Cardiac surgery

Since their invention, surgeons have used preoperative diagnostic imaging techniques such as MRI, CT, echocardiography, and angiography to prepare for cardiovascular surgery

and interventional cardiology. However, even with high resolution imaging capabilities it remains difficult to predict the actual anatomical structures for patients with congenital or other intra-cardiac defects, owing to great morphological diversity. Surgical preparation has a high associated risk for patients with a history of previous operations. Vessels can tear open and cavities can burst while scars are dissected. A realistic setting with lifelike heart dimensions provides an ideal platform for training surgeons.

MRI angiography and CT data have been successfully used to fabricate 3D models that are helpful in strategizing treatment paths, intraoperative orientation, and patient demonstrative guides since early 2000 (Sodian et al. 2007). By implementing SLA as a rapid prototyping method, researchers were able to model complex features in congenital heart disease (CHD) such as damaged pulmonary vascular tree (Ngan et al. 2006), complex vascular pathology, and intracardiac lesions (Sodian et al. 2007). Furthermore, FDM has also been used as a successful technique to model cardiovascular anatomy for various cases (Valverde et al. 2017). These studies served as proof of concepts for the use of rapid prototyping for cardiac surgery applications, achieving +95% accurate representation by the models (Noecker et al. 2006; Mottl-Link et al. 2008; Jacobs et al. 2008).

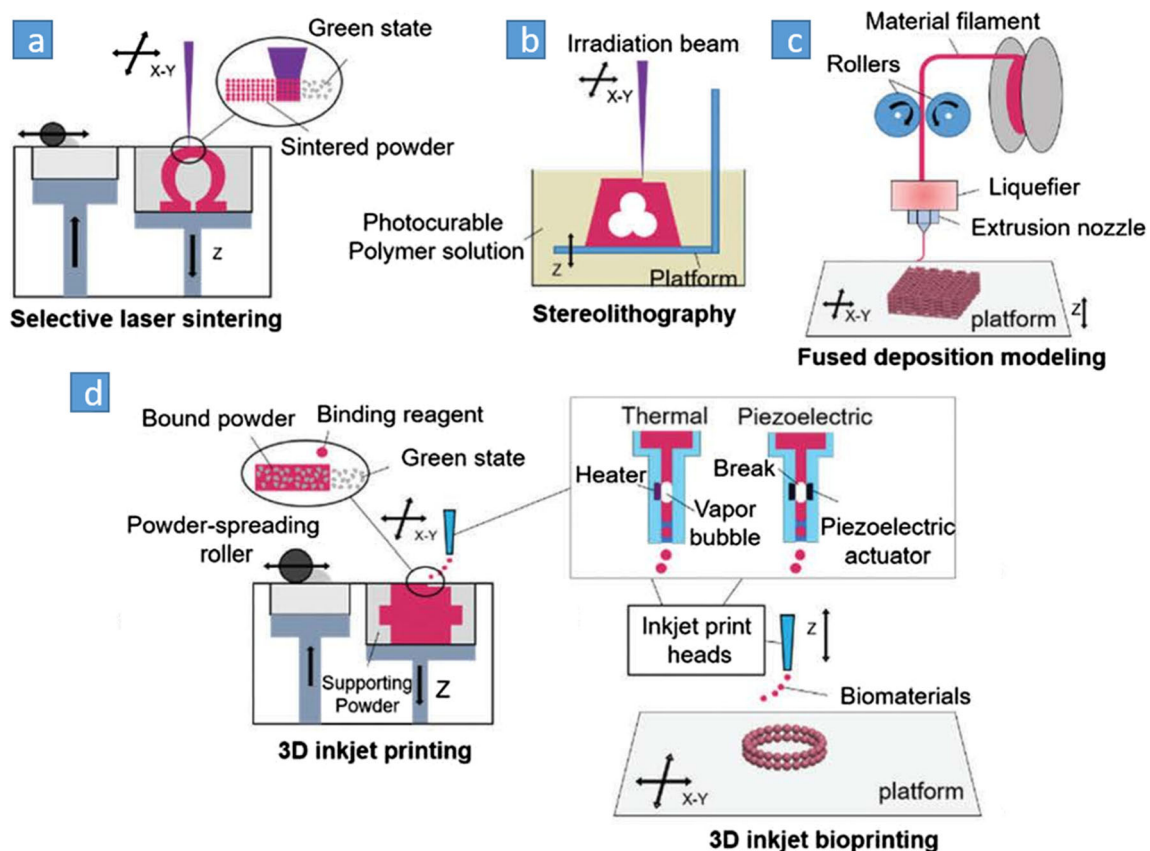


Fig. 2 Schematic representation of rapid prototyping techniques for surgery applications: (a) Selective laser sintering (b) Stereolithography (c) Fused deposition modeling (d) 3D inkjet printing (Park et al. 2016). (Copyright © 2016 Royal Society of Chemistry)

Several successes have achieved recreation of case specific 3D heart models from different imaging techniques. While most image sources are MRI or CT, these methods may involve intravenous contrast, sedation, and ionizing radiation. Contrastingly, 3D echocardiography has improved in resolution substantially with the development of new transducers and advancement of software and hardware; achieving higher resolution imaging without the drawbacks. For this reason, 3D echocardiography data has been tested as a suitable image source for 3D modeling (Olivieri et al. 2015). By converting 3D echocardiography image data into compatible files and 3D printing through rapid prototyping, models displaying ventricle septal defects and perivalvular leaks were successfully developed and were shown to be highly correlated to the 2D raw data.

Alterations to standard rapid prototyping techniques have enabled unique approaches to 3D modeling of cardiac structures. A novel rapid prototyping technique was developed, for example, using a powder and binder-based technique to fabricate lifelike models of exact aortic anatomy (Schmauss et al. 2012). This method was used as a postoperative approach to effectively assess decisions made in a diseased patient that had undergone a failed transcatheter aortic valve replacement. Another approach showed the use of the “drop on demand” 3D printing technique for evaluation of appropriate transcatheter percutaneous pulmonary valve implantation (PPVI) approaches (Schievano et al. 2007). While PPVI can overcome many disadvantages of surgery, it is limited to patients with a specific anatomy. The development of accurate 3D representations of such anatomies was shown to be effective in the cardiologists’ decision making.

Exploring methods to improve representation has also been of interest to clinical researchers. 3D modeling of cardiac structures can usually be hindered by complex morphologies which become more erratic in diseased tissue. Therefore, the use of techniques that can achieve sub-millimeter reconstruction is key for proper diagnosis and preoperative planning with the use of 3D printed models. One approach to generating solid 3D models with sub-millimeter resolution (accurately depicting complex 3D cardiac geometries) is combining high spatial resolution imaging (MDCT) with iterative closest point algorithms (ICP) (Greil et al. 2007). This enabled the reconstruction of STL heart models and cardiac segments utilizing a laser sintering technique with a mean surface distance of approximately 250 μm , which were successfully analyzed in comparison to standard techniques of assessment (echocardiography, angiography, etc.). This has shown how the development of algorithms to create 3D renderings from medical images is a critical variable towards building patient-specific reconstructions of individual cardiac structures.

Some approaches towards high fidelity replicas have taken advantage of different material properties to achieve soft or clear models of cardiac structures. By combining multi-slice

computed tomography data and SLA with *rubber-like* urethane and solid epoxy, flexible models of CHD cases were accurately fabricated. These models served for both planning innovative cardiac surgical procedures (Shiraishi et al. 2010), as well as effectively teaching multiple seminars on targeted surgical simulation of VSDs in the pediatric heart (Costello et al. 2015, 2014). The high-fidelity replicas were made by mixing a transparent plastic and a rubber-like material, which provided the freedom to cut with a scalpel blade while preserving structural integrity of the model. Towards similar training efforts, (trans-apical aortic valve replacement training), translucent heart models were effectively fabricated out of CT imaging data by using silicone, which allowed the trainees to see the stent valve throughout the exercise (Abdel-Sayed et al. 2009; Abdel-Sayed and Von Segesser 2011). This improvement was necessary as this procedure requires trainees to be able to see through the heart to visualize their performance. Current artificial heart models are usually opaque, as they are made of polyurethane, and thus are not ideal.

3.2 Neurosurgery

Use of rapid prototyping technology for neurosurgery simulation is still new and vastly unexplored due to the complexity of structures in the brain. In the case of preoperative planning in neurosurgery the aim is to find the safest approach that minimizes permanent brain tissue damage (Spottiswoode et al. 2013; Kettenbach et al. 1999). Since their development, medical imaging techniques such as MRI have been used by neurosurgeons to plan brain surgeries. Due to the excellent contrast of soft tissues, these images can display a clear distinction between the healthy tissue and that to be resected (Hirsch et al. 2000; Geerts et al. 2007). Up until recently surgical approaches were simulated in virtual reality. Recent advances in virtual surgical simulation for the brain using MRI imaging data and haptic devices have improved surgical outcomes by allowing surgeons to simulate the exact surgery on a computer and finalize the optimal approach (Lemole et al. 2007). But even with these simulation techniques, correct depth perception on a 2D screen is difficult, and these simulations do not allow realistic interaction with the anatomy, which only 3D printed models offer.

The first rapid prototyping proof of concept approaches to neurosurgery consisted of virtual simulations derived from MRI/CT data, followed by 3D printing of the anatomy for the rehearsal and refinement of the final surgical plan. In a recent study, a virtual reality pre-surgical simulation called interactive virtual simulation (IVS) in combination with 3D printed models demonstrated the use of rapid prototyping for preoperative planning and rehearsal in cases of skull base and deep tumors (Oishi et al. 2013). The many advantages of the use of this combination for pre-surgical planning included an

increased anatomical understanding for the complicated bone dissection necessary to achieve canals in skull base without any damage to surrounding tissue. Various novel approaches to the 3D printing of nervous tissue focus on developing methods to fabricate brain tissue models capable of incorporating cerebral circulation details.

Even though virtual surgical simulation has greatly advanced preoperative planning, it fails to provide the complete experience of rehearsing the surgeries or planning a surgical route with actual instruments. The need for considerable computer skills and hardware have also been limiting factors in widespread application. As presented above, initial efforts combined standard CT and MR angiography data to demonstrate the first application of 3D printing (SLA) for cerebrovascular biomodeling of patients with cerebral aneurysms and cerebral arteriovenous malformations (AVM) (Urso et al. 1999). These replicated vasculature models were solid in structure and displayed only the internal lumen structure, highlighted by contrast in CTA or by blood flow in MRA.

In a later study, 3D printed SLA models of cerebral aneurysms with parent and surrounding vessels were built from 3D CT scans and 3D rotational angiography data (Wurm et al. 2004). This data acquisition method enabled the fabrication small vessels, with a resolution of 0.4 mm. However, because the models were fabricated of a rigid synthetic resin, they were of very limited value in evaluating neck geometry, performing clipping simulation, and practicing dissection exercises. Therefore, while achieving higher resolution than previous works, these models did not aid in preoperative planning such as determining optimal patient head position.

Other works have focused on demonstrating the first 3D printed hollow models of cerebral aneurysms which could be practically used for preoperative planning and surgical training (Kimura et al. 2009). The 3D elastic vasculature model was fabricated using a rubber-like polymer from CTA data and MagicsRP software. UV light was used to cure the vessel walls while the uncured center part of the vessel cross-section was curetted away manually to make the vessels hollow. For surgical simulation, the models were immobilized with plastic clay in the direction of the surgical window, and the clipping procedure was performed under the operative microscope. Post-clipping, the lumen of the vessels was checked using a flexible vascular endoscope for patency of the parent vessel. To simulate the surgery in cases with complex, deep-seated vertebrobasilar aneurysms, the authors used a hard, 3D printed model with aneurysms, vessels, and a cranial base bone, also performing a craniotomy simulation to gain access to the aneurysms. This method allowed for the optimization of the surgical window location for clipping placement. Overall, this approach proved useful in preoperative planning and could also be an ideal tool for new surgeon training. However, the model fabrication took several days, and the lumen formation technique was not ideal.

Later in 2013, another approach to fabricating a hollow, clipable cerebral elastic model for surgical simulation demonstrated the first solid 3D model of an aneurysm and the parent artery using a FDM-based 3D printer (Mashiko et al. 2015). In this instance, the surfaces of the fabricated models were manually smoothed and dip coated with a layer of elastic silicone and hardener mixture. The silicone was allowed to harden for 6 hours, followed by dissolution and removal of ABS, resulting in hollow elastic models of the aneurysm. The advantages of this technique included lower cost and reduced fabrication time (14–24 hours). Also, because the hollowing was not performed by curettage, branched and complicated parent artery systems could be fabricated. The hollow elastic models also simulate the artery deformation that occurs during surgery. This simulation was performed preoperatively and aided the surgeon in choosing the optimal surgical approach and correct clip design (Fig. 3i–h).

Other efforts on developing standard techniques of rapid prototyping for neurosurgery have explored the implementation of new materials to achieve more realistic 3D models. Treatment of some cerebral aneurysms and tumors requires drilling of the temporal bone during skull base surgery, and although cadaver dissection has been the primary form of training in such cases, it has very limited accessibility. To address this, one case modified 3D skull base model using selective laser sintering (SLS), designing it to mimic surface details, inner bony structures such as the inner ear and air cells, artificial dura matter, cranial nerves, the internal carotid artery, and venous sinuses for surgical training (Mori et al. 2008). Materials such as silicone, sponge, and rubber fiber were used to model intricate and soft tissue structures. Two simulation surgeries were successfully performed on the model using ultrasonic bone curette or a high-speed drill.

3.3 Craniomaxillofacial surgery

The inherent complexity and variations in the craniomaxillofacial anatomy make reconstructive surgeries a challenging task. Software simulations in conjunction with high resolution 3D images have significantly improved preoperative planning by allowing the manipulation of images to simulate surgery. However, tasks such as realistic simulations of osteotomies, positioning of bone fragments, and assessment of intraoperative position and symmetry of deformed anatomy are difficult to accomplish with virtual reconstructions. Complications including improper assessment of deep skeletal contours of orbit and skull base, variability in the positioning of different facial components such as sagittal jaw and skull base relative to each other, and variations in craniomaxillofacial development, also demand the use of 3D printed biomodels.

There have been very few alterations to the basic techniques to rapid prototyping for craniomaxillofacial surgery.

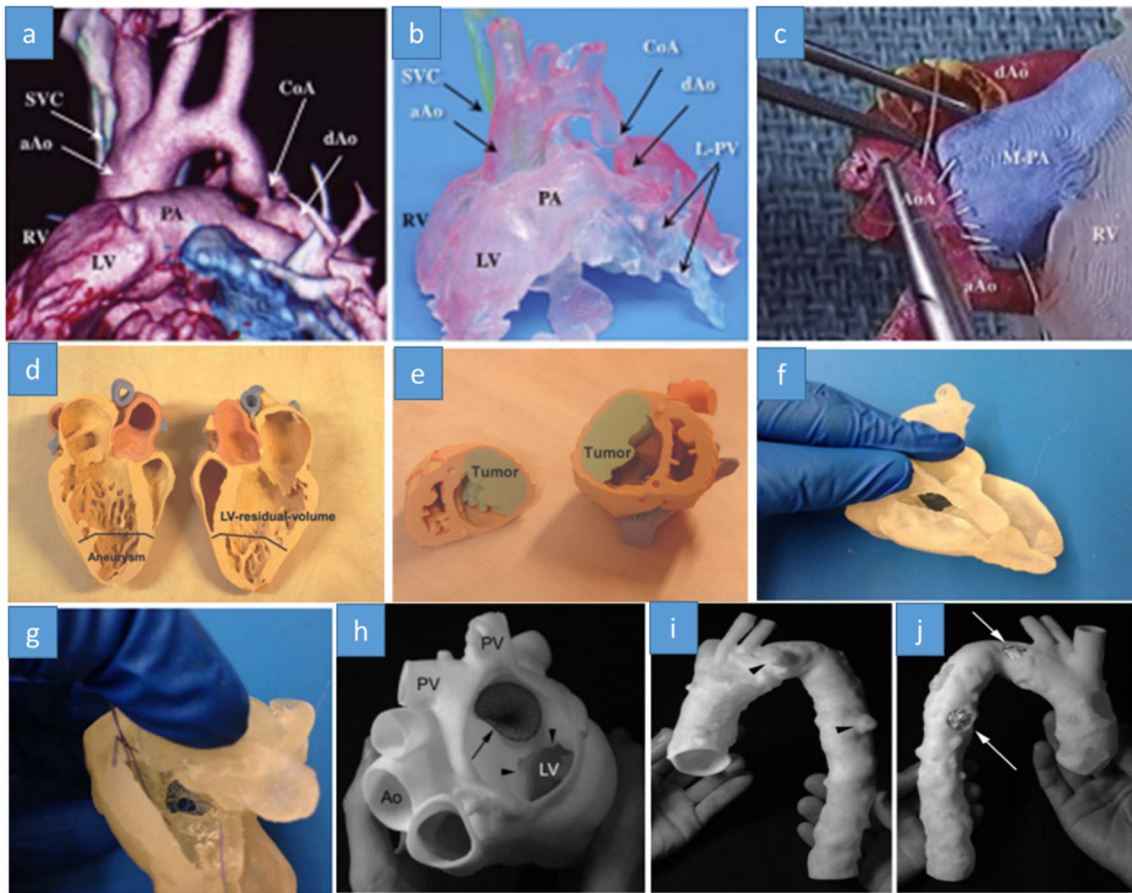


Fig. 3 3D printing for cardiac surgery. **a** and **b** CT data and 3D printed solid resin model of a 2 month old with isolated coarctation of aorta (Shiraishi et al. 2010) **(c)** Simulative surgery with rubber-like urethane model of 4-day old neonate with hypoplastic left heart syndrome (Shiraishi et al. 2010) (Copyright © 2010, Oxford University Press) **(d)** Model of a patient with aneurysm and LV-residual volume (Jacobs et al. 2008) **(e)** Massive cardiac tumor with infiltration to the right ventricular and tricuspid valve (Jacobs et al. 2008) (Copyright © 2008, Oxford University Press) **(f)** and **(g)** surgeon training

exercise with flexible 3D printed model – surgical right atriotomy revealing VSD location and suture placement around VSD lesion (Costello et al. 2014) (Copyright © 2014, SAGE Publications) **(h)** close up on left atrial disc of an amplatzer 35 mm ASD occluder (arrow) demonstrating no obstruction of the mitral valve annulus (arrowheads) (Kim et al. 2008) **(i)** and **(j)** anterior view of multiple aortic ulcerations and posterior view of thoracic endoprosthesis placement (arrows) (Kim et al. 2008) (Copyright © 2008, American Heart Association, Inc.)

Minor deviation from gold standards has been implemented to achieve more accurate models. A distinct approach used cone beam CT (CBCT) instead of the standard multi slice CT (MSCT) to fabricate 3D models using an SLS technique for two patients, both yielding favorable results (Adolphs et al. 2013). For one patient with severe skeletal class III malocclusion in an edentulous upper jaw, the 3D model clearly demonstrated the need for a two-jaw correction to achieve alignment, whereas for the other patient with a severe class III malocclusion due to a bilateral cleft lip and palate, maxillary distraction was performed after planning the procedure on the model. In yet another demonstration, 3D printing was used for implant pre-shaping in the cases of bilateral craniomaxillofacial post-traumatic deformities, instead of simply serving as a model reference (Cui et al. 2014). In this study, 3D printed SLS models of the skull were fabricated and a rehearsal surgery

was performed to discover the location, reduction direction, and shift distance of the osteotomy. Pre-shaping of the titanium plates or mesh was done on the models before implantation. Satisfactory aesthetic and functional results were achieved in all the cases with no post-operative complications (Fig. 5a). This approach has also been implemented to pre-bend titanium mesh implants for orbital floor fractures and to intraoperatively guide the correct placement of the implant (Kozakiewicz et al. 2009; Mustafa et al. 2011). Complex orbital anatomy makes intraoperative titanium mesh shaping and cutting very difficult, and results in less than satisfactory results in terms of final shape. The models helped in achieving the desired shape of the implant preoperatively and resulted in improved surgical outcomes in a shorter operating time. Improvement of vision was demonstrated by the elimination of diplopia and enophthalmos.

The testing of rapid prototyping techniques has also been implemented for ear surgery. Tympanoplasty is especially difficult because of the anatomical complexity of the ear. Safe surgery to restore good hearing in cases such as atresia is difficult even after using CT imaging and virtual reconstruction. To address these challenges, Suzuki et al (2005) demonstrated the use of selective laser sintering (SLS) to fabricate a 3D model for surgical simulation of a malformed ear. Temporal bone models of congenital aural atresia were prototyped, and conventional surgical instruments were used to dissect the models as a part of surgical planning and rehearsal. The SLS models performed better than stereolithographic models as they permitted the use of a surgical drill, such as that used on real bone, and could simulate other surgical procedures such as dissection. This finding was further confirmed by various reports on building 3D printed models of middle and inner ear anatomy to improve anatomical understanding of trainees (Suzuki et al. 2004a, b). In the enlarged models, the mastoid air cells had already been dissected, exposing sinodural angle, surgical dome, endolymphatic duct, and the sigmoid sinus. An enlarged model of the osseous labyrinth was also shown. The in-depth three-dimensional anatomical knowledge obtained from these models could greatly assist trainees in understanding the complexity of tympanoplasty.

4 Case studies

While there have been gradual improvements in the techniques used for rapid prototyping of physiological structures, most of the medical studies performed on the use of 3D printed models for preoperative planning and surgical training have focused on providing a proof of concept for morphologies of specific diseased tissues or organs of interest. The following is a summary of case studies that have focused on showing the feasibility of the rapid prototyping technique as a method for preoperative planning or training and whose novelty lies on the organ structure and not the technique itself.

4.1 Cardiac surgery

4.1.1 Congenital heart disease (CHD)

Congenital heart disease (CHD) is a common cardiac pathology and occurs in 0.8–1.2% of all live births worldwide, 50% of which are ventricular septal defects (VSD) (Costello et al. 2015; Hoffman and Kaplan 2002; Reller et al. 2008). Surgical planning and intraoperative orientation is difficult in CHD reoperation cases due to excessive scar tissue and fibrous strands which make it challenging to identify anatomical structures and dimensions. Congenital heart disease (CHD) is associated with complex intra-cardiac anatomy, due to the

variability of defects which may be present. The complexity of anatomical structures in CHD cases warrants the need for 3D printing to understand the spatial organization, plan the surgery preoperatively, carry out surgical simulations, and guide the surgeons during operation. Current approaches for surgeon training, including pathological specimens, pictorial 2D images, and animal models, fail to provide a sufficient understanding of specific scenarios. The accurate visualization of intra-cardiac structure is essential for the diagnosis and treatment of such conditions. Greil et al. (2007) demonstrated the ability to fabricate accurate 3D models for CHD cases, utilizing high spatial resolution imaging (MRI/MDCT) of patient anatomy, accurately depicting complex 3D geometries such as connections of the atria, ventricles, and great arteries of a criss-cross heart, as well as fine ventricular trabeculations and the proximal and distal course of the main coronary artery. However, small cardiac structures such as papillary muscles, semilunar valves, and atrioventricular valves were not captured due to limited image resolution caused by blood pooling and motion artefacts. Surgeons performed a simulative Norwood procedure on a 4 day old neonate with hypoplastic left heart syndrome (Fig. 3a–c). Noecker et al. (2006) fabricated rigid and flexible models of 11 patients with and without CHD, capturing the complex arch anatomy that is present in CHD cases. These powder and starch-based inkjet printed models provided tactile and spatial representation and could be used for medical device development and preoperative testing.

Mottl-Link et al (2008) demonstrated the clinical application of a powder-based 3D printed (inkjet) model of a CHD case by using it intraoperatively during a high-risk procedure. With the aid of the replica, pathological localization of highly abnormal structures and coronary arteries was easily achieved, allowing the closure of a large ventricular septal defect. In another instance of preoperative planning, Vranicar et al. (2008) fabricated hand-held models of CHD cases to evaluate the abnormality of the great arteries. 3D printed models of cardiovascular anatomy of 9 patients with aortic coarctation and 3 patients with vascular rings were constructed. The clear depictions of pathologies in the fabricated replicas aided in surgical and transcatheter intervention.

Pulmonary atresia with ventricular septal defect (VSD) and major aortopulmonary collateral arteries (MAPCAs) is an uncommon form of cyanotic congenital heart disease in which the native pulmonary arteries are highly hypoplastic or even absent. In this case, the corrective surgery aims to repair intra-cardiac defects, connect the MAPCAs to the pulmonary arterial system, and form continuity of right ventricle to pulmonary artery. In this process, identification and isolation of MAPCAs is one of the most challenging tasks.

In some cases of CHD in which native pulmonary arteries are highly deficient, identification and isolation of major aortopulmonary collateral arteries can prove to be highly

difficult without 3D models. Using CT angiography and 3D printing, Ngan et al. (2006) built accurate replicas of vascular anatomy that proved very helpful for preoperative planning and intraoperative success. The authors found that 96% and 93% of the major aortopulmonary collateral arteries identified during surgery and conventional angiography, respectively, were accurately represented by the models. Moreover, surgeons found the models to be highly useful in visualizing the vascular anatomy.

Sodian et al. (2007) used MRI angiography and CT data to fabricate stereolithographic models of cardiovascular anatomy of 2 pediatric patients, one with a left retro-esophageal abnormal subclavian artery and a right descending aorta and the other with a ventricular septal defect. These replicas were used for surgical planning and intraoperative orientation and were found to greatly facilitate both. The authors report that such models may not be necessary in every case, but when incorporated can aid in anticipating intraoperative problems by providing better anatomical information. Selection of the correct segmentation values during MRI and CT image processing was identified as a bottleneck of this technique. In yet another study, Sodian et al. (2008a) evaluated 3 cases of pediatric cardiac transplantation in patients with univentricular heart by using stereolithography to fabricate 3D printed models from MRI imaging data. The patients had undergone multiple corrective procedures and had relatively unpredictable anatomy. The 3D replicas assisted in preoperatively planning the heart transplantation by providing specific dimensions, spatial organization, and special requirements for the donor heart. In a similar work by Oliveri et al. (2015), fabrication using a polyjet printer from 3D echocardiography data (instead of the much established MRI or CT) provided accurate 3D printed models of congenital cardiac defects such as ventricular septal defects and periprosthetic aortic valve leaks. Comparisons between the 3D digital model and the physical model showed the congruency between the two, thus establishing that echocardiography imaging data can be reliably used for bio-modelling.

4.1.2 Coronary artery bypass grafting (CABG)

Coronary artery bypass grafting (CABG) is a process by which a healthy artery or vein from the body is grafted to the patient's blocked coronary artery, bypassing the blocked portion of the coronary artery and creating a new path for oxygen-rich blood to flow to the heart muscle. A large patient population with previous CABG have reported significant aortic stenosis (Odell et al. 1996). Reoperation on such patients for aortic valve replacement has a high mortality rate owing to the unpredictable anatomic structure (Fighali et al. 1995; Collins and Aranki 1994). Repeat sternotomy, an incision on the sternum or breastbone, entails the risk of dissecting the patient's vein or internal mammary graft from previous surgery. Sodian et al.

(2008b) fabricated a 3D printed SLA model of cardiovascular anatomy of a patient with symptomatic aortic valve stenosis and previous coronary bypass grafting. The model helped locate the bypass grafts and other structures intraoperatively and helped in opening the sternum without any damage.

4.1.3 Ventricular aneurysmectomy and reshaping

Alterations in ventricular volume and shape, along with reduced contraction of anterior wall and septum, are common conditions post anterior myocardial infarction (Zardini et al. 1993). Such ventricular dysfunction leads to aneurysm formation, which may finally lead to congestive heart failure (CHF). The corrective methods for such cases involves surgical resection of the aneurysm and ventricular reshaping. There are several techniques for ventricular reshaping, such as volume reduction (only if a dyskinetic scar is present), or surgical repair of the postinfarction dyskinetic aneurysm (Jatene 1985). Ventricular rest volume and geometry are important parameters for correct reshaping of the ventricle, and any mistake directly affects ejection fraction and stroke volume. For this particular application, Jacobs et al. (2008) fabricated powder-based 3D printed (inkjet) models of cardiovascular anatomy for 2 patients with ventricular aneurysms and used them to determine the ideal resection lines for aneurysmectomy as well as the shape of the residual ventricle post-reconstruction. Using the left ventricle (LV) aneurysm 3D model, reshaping of the left ventricle with a sufficient LV volume was easily accomplished (Fig. 3d).

4.1.4 Cardiac tumors

Primary cardiac tumors are extremely rare but have the potential to be fatal. Complete surgical resection is required for improved survival (Murphy et al. 1990). Echocardiography, MRI, and CT are all useful in determining the extent of infiltration of the tumor (Kaminaga et al. 2003), but because of the beating heart, radical complete resection is rarely possible. Additionally, due to the rarity of cardiac tumors, many surgeons have limited experience in their treatment. A 3D model of the target area could help in identifying the optimal resection volume, thus enabling maximal organ preservation. Jacobs et al. (Jacobs et al. 2008) used an inkjet powder-based technique to 3D print a cardiovascular model of a patient with cardiac fibroma and used it to plan the tumor resection procedure. Owing to the massive tumor infiltration to the tricuspid valve, the authors decided to access the tumor through the right ventricle instead of the right atrium (Fig. 3e). A complete tumor mass reduction along with tricuspid valve replacement was achieved. In a similar work, Schmauss et al (2013) built a 3D printed SLA model of a primary cardiac tumor on the right ventricular wall and successfully used it to define the infiltration of the tumor and plan for its resection.

4.1.5 Cardiovascular

The past few years have seen a tremendous rise in cases of catheter based treatment for congenital as well as structural heart diseases. Both structural modifications and novel device implantation have been shown using catheter based treatment. Cardiac valve interventions can be very complex and intra-cardiac navigation of delivery systems requires an in-depth understanding of spatial relationship of the anatomy, which varies from patient to patient. Ablation procedures in electrophysiology, which are done as intra-cardiac therapeutic procedures, also require thorough understanding of the patient's cardiovascular anatomy.

Using CT angiography data and fused deposition modelling, Kim et al. (2008) fabricated 3D printed models of cardiovascular anatomy for 4 cases: congenital muscular VSD, fenestrated ASD with large atrial septal aneurysm, prosthetic mitral valve perivalvular leak, and thoracic aortic pseudoaneurysm and ulcerations. For the VSD case, the 3D replica was used to simulate different approaches to crossing the VSD using a catheter, including superior vena cava, inferior vena cava and retrograde aortic approaches. The retrograde approach was found to be optimal in minimizing bending and maximizing primary and secondary bends of the catheter. A 12-mm Amplatzer muscular VSD occluder device was chosen for closing the defect. For the second case of ASD and aneurysm, the 3D replica was used to choose a 35 mm Amplatzer device to cover all fenestrations. Various catheters were placed in the model to finalize the approach of crossing the fenestration to place the device and to select the make of the catheter. For the prosthetic mitral valve perivalvular leak, the 3D replica was used to discover the distance needed to be travelled by the transseptally placed delivery catheter, the angular orientation required to reach the defect, and the size of the occluder device. In the last case, the 3D replica helped in identifying the number and precise locations of pseudoaneurysms and ulcers. A 31 mm diameter by 15 mm length gore TAG thoracic endoprosthesis was placed that covered both the aneurysm and ulcerations (Fig. 3h–j).

After the replacement of the ascending aorta and aortic arch, and re-implantation of the supra-aortic vessels; development of a false aneurysm is regarded as a severe complication (Mohammadi et al. 2005). The standard treatment for this condition has been surgical, with a high mortality rate (Mohammadi et al. 2005). The other option uses endovascular interventional techniques but is often complicated (Angeli et al. 2004). Decision-making is difficult in this scenario, as important information about aneurysm dimensions, its relationship to supra-aortic arteries, and the shape of the opening between the aneurysm and aortic lumen are difficult to gauge. Sodian et al (2009) used SLA to print a model of aortic anatomy of a patient with aortic pseudoaneurysm after replacement of the ascending aorta. The model helped in

fabricating a custom-made occluding device and in simulating the intervention procedure. Using the 3D replica, surgeons could identify the dimensions of the pseudoaneurysm as well as the shape of the opening between the aortic lumen and false aneurysm. Due to the slit shaped opening, the occluder device had to be custom built, as the Amplatzer commercially available devices are round in shape. This conclusion likely would not have been made without the printed model.

4.1.6 Transcatheter AVR

In recent years, transcatheter aortic valve replacement (TAVR) has become a promising alternative to open surgical methods. However, the standard outline for preoperative planning for such procedures is largely missing. Schmauss et al (2012) report a case of a 70 year old patient with severe aortic stenosis and a porcelain aorta who was referred for transcatheter aortic valve replacement but died during operation due to ischemia. The authors, using powder and binder-based technique (inkjet), did a postoperative 3D fabrication of the aortic anatomy of the patient and used it to re-evaluate the course of surgery. The model assisted in the discovery that the heart valve should be placed deep into the aortic annulus in cases with a small and inelastic sinus of Valsalva, preventing the occlusion of the coronary ostia and improving the outcome of such surgeries.

4.1.7 Transcatheter percutaneous pulmonary valve implantation (PPVI)

The number of patients requiring surgical replacement of the pulmonary valve or conduit continues to increase. Pulmonary valve abnormalities are most common in patients with repaired congenital heart disease as pulmonary incompetence can occur in such cases. Scheivano et al (2007) showed the use of the “drop on demand” 3D printing technique for transcatheter percutaneous pulmonary valve implantation (PPVI), which can overcome many disadvantages of surgery but is limited to patients with a specific anatomy. This procedure requires an exact size, shape, and physical properties of the implantation site in order to safely anchor the valved stent. Preoperative planning and patient screening is even more crucial due to large variation in 3D geometry and the relationship of the right ventricular outflow tract (RVOT) and pulmonary trunk among patients. The authors used 3D printed rigid models of RVOT and pulmonary trunk for the patient selection process and showed that use of printed models resulted in a more accurate selection as compared to the MRI alone.

4.1.8 Left atrial appendage closure

Left atrial appendage closure, a treatment to reduce the risk of blood clots entering the bloodstream and causing stroke in non-valvular atrial fibrillation patients, is currently done using

the Watchman device under fluoroscopic and transesophageal echocardiographic guidance. MDCT offers a 3D dataset with better resolution but can still result in procedural failure owing to the complex morphology. Otton et al (2015) fabricated a 3D printed (polyjet) patient-specific model to guide a left atrial occlusion surgery using the Watchman device. The model was fabricated using a rubber-like material to simulate atrial mechanical properties. Watchman devices of varying sizes were placed in the model and anatomic deformation tests were performed. This exercise helped in selecting the correct dimension of the device to avoid any post-operative complications.

Ensuring patient safety and improving surgical success rates are the ultimate goals for any surgeon. Fueled by these motives, the field of surgical training has seen widespread acceptance of simulation-based training curriculum. Surgical simulation creates a safe environment for practice and error that maximizes learning (Akaike et al. 2012). In spite of the widespread acceptance of the concept, its application is still scant in critical areas like congenital heart disease surgeries. Below we discuss various specific applications of 3D printing for surgeon training in the field of cardiac surgery.

4.1.9 Ventricular septal defect - pediatric heart

Pictorial images and 2D echocardiography data of CHD prove insufficient for users who lack the real-world 3D perspective. Animal models with structural defects are limited, and do not provide an accurate representation of CHDs in humans. Costello et al. (2015, 2014) conducted multiple teaching seminars on targeted surgical simulation of VSDs in the pediatric heart with 3D printed (polyjet) replicas of 5 common VSD subtypes. The models were made of a plastic and a rubber-like material mixture, and could be cut with a scalpel blade without damaging the structural integrity. Although limited MRI image resolution prevented accurate depiction of the heart valves in the models, all participants in the seminar reported significant improvement in knowledge acquisition, knowledge reporting, and structural conceptualization (Fig. 3f–g).

4.1.10 Trans-apical aortic valve replacement

Trans-apical aortic valve replacement (AVR) is a growing technique that requires a high level of surgical skill. Existing training approaches have been similar to the aforementioned techniques used in conventional CHD training. For trans-apical AVR training, the trainees must be able to see through the heart to visualize their performance. Current artificial heart models are usually opaque, as they are made of polyurethane, and thus are not ideal. Abdel-Sayed et al. 2009; Abdel-Sayed and Von Segesser 2011) found a solution to this problem by using CT imaging data to fabricate translucent heart models made of silicone which allow the trainee to see the stent valve throughout the exercise.

4.2 Neurosurgery

4.2.1 Brachytherapy

Poulson et al. (1999) described the use of 3D printed models for neurosurgery planning as early as 1999. A fabricated stereolithographic model for a patient diagnosed with an orbital tumor was used to assist an orbital brachytherapy. Brachytherapy is an advanced cancer treatment where, using hollow plastic or metal needles, radioactive seeds or sources are placed in or near the tumor, giving a high radiation dose to the tumor while reducing the radiation exposure to the surrounding healthy tissues (Tyl et al. 1997). This is usually done under direct visualization in cases where the tumor is palpable. Correct needle placement is critical as the radiation dose from the seeds falls off rapidly. Incorrect needle placement will result in “hot” or “cold” spots causing complications in healthy tissues, such as necrosis. Application of brachytherapy to orbital tumors poses two specific challenges: first, the tumor is not visually obvious so accurate needle placement is difficult; second, the needles may damage the optic nerve. Using the 3D printed replica, the authors determined important pre-surgical questions, including the number and length of the needles needed to cover the tumor, the trajectory of needle insertion, and the separation between the needles being used (Fig. 4a–b).

4.2.2 Skull base surgeries

Muller et al (2003) fabricated SLA and SLS models of patients to assist in the planning of skull base procedures. Exposure to the lesion through precise planning is critical for surgery, and many standard approaches to different skull base regions have been demonstrated (Fisch 1985; Al-Mefty et al. 1987; Bertalanffy 1991). Lesions which cannot be reached or exposed through standard approaches are often encountered, and dealing with such cases requires further understanding of the patient’s anatomical variations. In this study, a standardized approach using only imaging (MRI or MDCT) was found to be ineffective. The skull base lesion and surrounding structures were reconstructed in 3D on a computer screen, using Materialize 3D software. These models also aided in determining the surgical route and provided perspective for deep tumors. Skull base tumors require tailoring of procedures to individual patients with respect to craniotomy, bone resection, spatial composition of the target, and the surgical trajectory. This combination approach proved very useful for these processes (Fig. 4d–g).

4.2.3 Lesion near motor cortex

Spottiswoode et al. (2013), using powder based inkjet printing, fabricated 3D printed brain models for two patients with lesions in proximity to the motor cortex. They also attached the fMRI

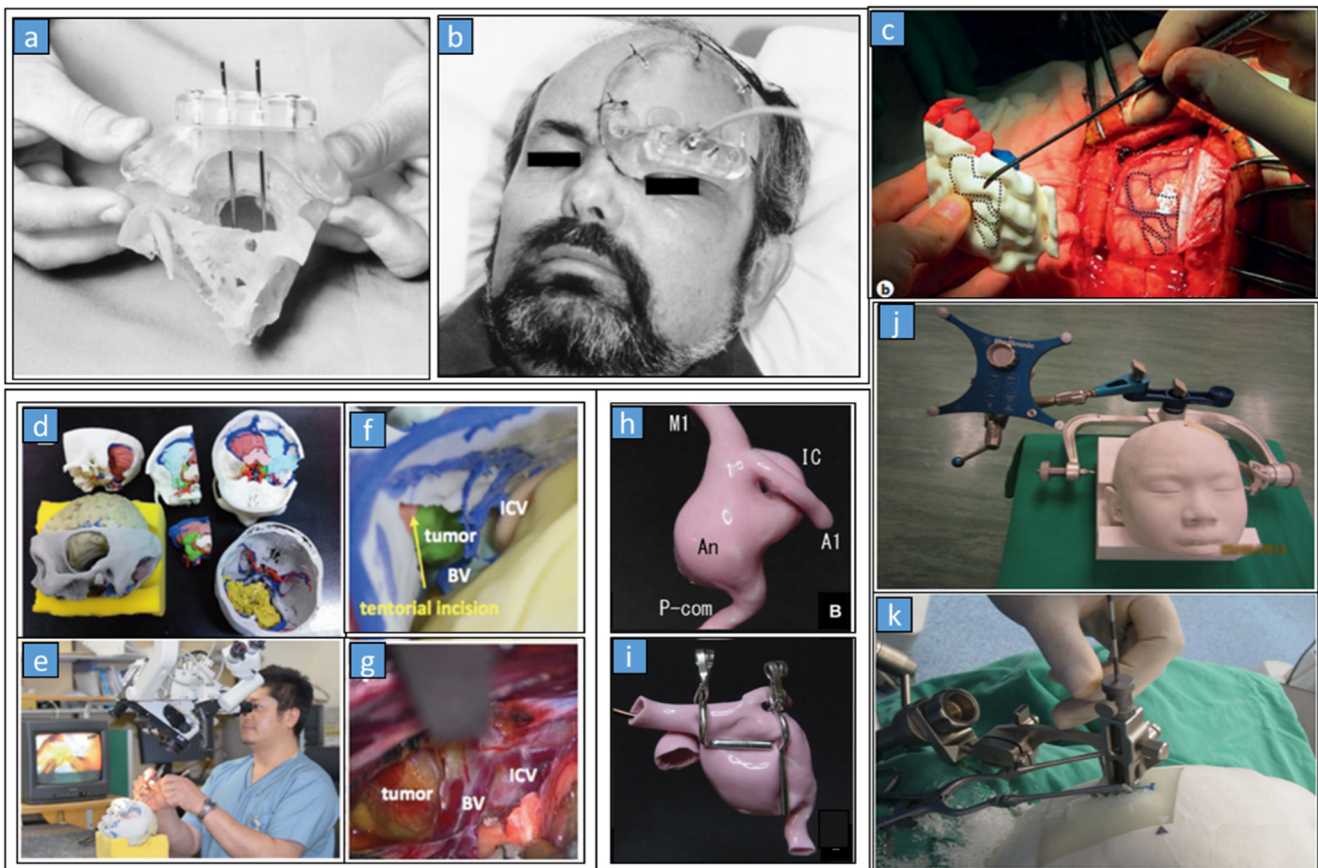


Fig. 4 3D printing applications in neurosurgery. **a–b** SLA biomodel for brachytherapy with template and needles and the patient with the template (on the right) (Poulsen et al. 1999) (Copyright © 1999 Elsevier Science Inc.) **(c)** 3D printed model showing lesion in blue and fMRI region in red and the corresponding features shown intraoperatively (Spottiswoode et al. 2013) (Copyright © 2013, Karger Publishers) **(d–g)** 3D printed color models of cerebrovascular anatomy; surgical simulation using model; tumor seen in the model and corresponding view intraoperatively (Oishi

et al. 2013) (Copyright © 2013, American Association of Neurological Surgeons) **(h–i)** Flexible model of left internal cerebral artery aneurysm and simulation of angioplastic neck clipping with 2 fenestrated clips (Mashiko et al. 2015) (Copyright © 2015 Elsevier Inc.) **(j–k)** 3D printed model of a patient with deep seated tumor and with image guidance frame in place for surgical simulation; tissue biopsy in progress during surgeon training (Waran et al. 2014a) (Copyright © 2014 Association of Program Directors in Surgery. Published by Elsevier B.V.)

volumes to the 3D printed models to get a clear indication of proximity of functionally eloquent areas to the tumor. This additional information can help surgeons plan the safest surgery route. The model showed detailed grey matter surface features, extent of the tumor infiltration, and gyri for intuitive navigation compared to actual brain morphology (Fig. 4c). The model fabricated in this study was found to have the appropriate dimensional accuracy (x,y,z spatial resolution of 0.042mm, 0.047mm, 0.089mm, respectively) to be useful in neurosurgical planning as well as training purposes. These models can also be used to facilitate communication with patients, in the explanation of the surgical procedure and associated risks.

4.2.4 Cerebrovascular

Cerebral aneurysm surgery is another major class of neurosurgery that requires thorough understanding of both the shape of the aneurysm and its relationship with the parent artery, cranial nerves, brain, and bones. The standard technique for open

cerebral aneurysm surgery is microsurgical clipping, wherein a small metal clip is used to stop the blood flow into the aneurysm. However, the use of endovascular embolization has also recently increased (Gnanalingham et al. 2006). Cases unsuitable for endovascular intervention are referred for clipping surgery and are usually complex and require in-depth understanding of the anatomical structure, effective planning, and practice. The diagnostic techniques to achieve the thorough understanding required for clipping surgery have evolved from cerebral angiography, wherein dyes and X-rays were used to visualize the blood flow patterns in brain, to high resolution techniques like CT angiography and MR angiography that also allow virtual 3D reconstruction of the images. Many researchers have exploited this advantage to demonstrate applications of virtual surgical simulation in neurosurgery (Futami et al. 2004; Satava 2001; Stadie et al. 2008). The cerebral aneurysms were found to be captured accurately by the 3D printed models and demonstrated the relationship of the vasculature to the skull base. Clipping was simulated on

the printed model, and surgeons found that they could optimize the patient positioning for surgery by manipulating the model to find the best angle of approach. However, vessels less than 1mm in diameter could not be fabricated using this method. The 3D printed models assisted in surgical planning, selection of the correct treatment (i.e clip or coil application), evaluation of the neck of the aneurysm, and selection of the best clip positions during surgery. The accuracy of the vascular models was found to be satisfactory when compared to the intraoperative video. Others have also fabricated rigid anatomical models validating the use of 3D printing for intracranial aneurysm biomodelling and confirming its feasibility for this application (Erbano et al. 2013; Xu et al. 2014).

4.2.5 Cerebral tumors

The cavernous sinus (CS) is comprised of the venous plexus, multiple cranial nerves, and the internal carotid artery. Thus, it is a key location for skull base surgery owing to the many intracranial pathologies that can occur in this region. Another such interesting region is the temporal bone that contains inner ear structures, cranial nerves, and the internal carotid artery.

Waran et al. (2014a, b; 2015) published multiple reports using 3D printing for simulating neurosurgical procedures. In their first report, patient head models with deep-seated small thalamic lesions were prepared using MRI and CT data and used for educating trainees on patient positioning in relation to pathology, utilization of navigation systems for cranial surgery, target selection, and surgical planning. The simulation included creating a burr hole in the skull followed by a biopsy on the underlying tumor. Medtronic S7 and BrainLAB Kolibri navigation platforms were used for navigation related steps. It was possible to load all imaging information onto both platforms and subsequently register the models as if the trainees were operating on a real patient (Fig. 4j–k). In a second report, the authors used similar 3D printed models for surgical training in navigation and planning of skin flap, to performing initial steps in a craniotomy and simple tumor excision. Most recently, the authors used a similar model for simulating third ventriculostomies and pineal biopsies for hydrocephalus secondary to a pineal tumor. In each of these cases, the model was fabricated using patient MRI and CT data. These models allowed endoscopic intraventricular biopsy training in addition to basic craniotomy procedures. The authors concluded that 3D printed models provide standardized and reproducible procedures, allowing candidates to repeat steps until they are confident, and thus improving the surgical training experience.

4.3 Craniomaxillofacial surgery

4.3.1 Maxillo-facial

Maxillofacial surgeries involve the region of upper jaw, nose, eye sockets, and the face. The earliest works on maxillofacial preoperative planning using 3D printing can be traced back to the late twentieth century. In 1998, Kermer et al. (1998) fabricated 3D printed models using SLA with CT data from patients suffering from acute maxillofacial trauma and used them for preoperative planning. Depending on the condition of the traumatized patients, primary treatment may be delayed in the favor of intensive care, and this time can be utilized to plan and rehearse surgery on 3D printed models for improved outcomes. In all of the patients treated in this study, the intraoperative situation was adequately captured by the 3D printed models and simulation surgery helped in better adjustment of mini or micro plates, resulting in satisfactory functional and aesthetic results. As an additional remark, the authors advised against the use of 3D printing for cases of very small fragments in the midface fracture due to the disconnected nature of the anatomy. Around the same time, Santler et al. (1998) published a cumulative report of their work with 3D printed SLA models for preoperative planning from 1988 to 1997. They found that in the case of congenital malformations the models helped in the precise diagnosis of the deformity whereas simulation surgery allowed prediction of intraoperative problems beforehand. In the cases of trauma, osteoradionecrosis, and osteomyelitis, the size, shape, and localization of the defect determined the transplant donor site and 3D printed models greatly facilitated this process. The models helped in exact jaw positioning in patients suffering from dysgnathia and allowed better planning for asymmetrical malformations. For patients suffering from severe alveolar crest atrophy, exact bone measurements on the 3D printed models helped in deciding whether bone transplants, dental implants, or a combination would be ideal. Also, rehearsing the surgery on the models allowed perfect implant positioning in relation to the opposite jaw. Overall, the authors believed that 3D printing facilitated precise diagnosis and correct surgical approach selection, and reduced operation time. In another work, Sinn et al. (2006) demonstrated the application of 3D printing (SLA) to fabricate custom adaptation of internal distracter device to be placed at the level of the zygomatic body and arch of a patient suffering from Cruzon's disease with severe hypoplastic maxilla. Custom-made devices are most useful where the already complex anatomy is further distorted as they can help avoid some of the problems like mechanism failure or loosening of the device due to inadequate bone stock. The 3D printed SLA models helped identify the area of greatest bone stock prior to surgery so that the device could be placed in the area of maximum bone.

The surgical training reports in craniomaxillofacial surgery have been confined to surgeries related to the ear. The complex three-dimensional anatomy of the temporal bone, along with its close association with neurovascular structures, requires extensive skill and experience. The established training module utilizes cadaveric temporal bones, but such specimens for trainee dissection have limited accessibility with significant costs of procurement (Longfield et al. 2015). 3D printed temporal bone models are a lucrative substitute to this conventional training approach.

4.3.2 Mandibular

Mandible reconstruction is a very complex procedure owing to the intricate geometry, presence of connected muscles which act in different directions, position of condyles in the glenoid fossa, and occlusion. Reconstruction is needed after partial resection and continuity defect, and is usually done with a titanium bone plate followed by an autogenous bone graft at a later stage. The bone graft allows dental rehabilitation and also provides aesthetic and functional restoration to the face. 3D printing is useful in providing the anatomical detail and the flexibility to physically carry out surgical procedures on models before the actual surgery. Multiple authors have demonstrated its relevance to mandibular reconstruction post tumor resection (Cunningham et al. 2005; Robiony et al. 2008). The focus of the treatment was to resect the tumor and preserve the form of the mandible. The 3D printed SLA models of the mandibular anatomy based on patient CT data allowed prefabrication of contour reconstruction plates, which in turn provided a more conservative surgical approach (Fig. 5b). The biggest disadvantage of 3D printing models was the added time and cost. In addition, Robiony et al. (2008) presented another mandibular application of 3D printing for class II dentofacial deformities where the 3D model was used to plan the elongation of the hypoplastic mandible in the desired occlusion. Previously, Gateno et al. (2000) had developed a protocol using virtual reality to simulate distraction osteogenesis of the mandible, and the authors used this to plan the correct elongation vector axis. After virtual evaluation of the functional and aesthetic aspects, a stereolithographic model of the surgical solution was prepared and used for intraoperative guidance. Good aesthetic and occlusal results were seen (Fig. 5c–e). In another demonstration, Sinn et al. (2006) used 3D printing to plan and create a custom HTR implant for the left mandibular body of a patient suffering from hemifacial microsomia, a congenital disorder which affects the development of the lower half of the face, usually including the ear, mouth, and mandible. In this case, the 3D printed model helped in constructing the implant to exactly match the contour of the deformed left mandibular body. Satisfactory aesthetic and functional results were observed and no radiographic evidence of implant migration or bony resorption beneath

the implant were found in the 5 year follow-up. Zhou et al. (2009) reported similar use of 3D printing in another case of unilateral hemifacial microsomia. The left jaw of the patient was less developed than the right. CT data showed the hypoplastic left mandible with wasting soft tissue and thinning skin and fat of the left cheek. As a standard procedure in unilateral deformities, the image of the right mandible was mirrored to the left using computer aided design (CAD) to restore the facial symmetry. The 3D printed model of the patient's mandibular anatomy helped in understanding the deformity and in deciding the best surgical treatment path. Satisfactory results were achieved. Oliveira et al. (2008) showed the use of 3D printed (SLA) biomodels in the surgical planning for two cases. One patient, suffering from partial mandible destruction due to a gunshot wound, had previously been implanted with a titanium plate to restore facial symmetry. In this surgery, the 3D printed models were used to determine the volume, length, and angulation required of the free flap obtained from autologous peroneal bone. A second patient, with ameloblastoma in the mandible, underwent tumor resection followed by autologous peroneal bone graft implantation. The 3D printed model helped in understanding the exact defect dimensions and positioning to determine the general morphology of the implant. Complete restoration of the defect and biofunctionality was seen for both the patients. Similar work on ameloblastoma cases in the mandible has been shown by other authors (Sannomiya et al. 2008; Cohen et al. 2009). In addition, Cohen et al. (2009) demonstrated the use of a 3D printed model as a template for iliac crest bone graft in second stage reconstruction where a comparison between the template and the bone graft revealed that the bone graft was short. This allowed the surgeons to plan appropriately, and a few bony fragments were fixed to the bridging plate instead of a monoblock.

4.3.3 Craniofacial

The earliest reports of 3D printing in craniofacial surgery date back to the late twentieth century. Bill et al. (1995) published a report in 1995 showing application of 3D printing for reconstruction of severe skull defects. With fabricated models of calvarial defect and the original skull with the defect, the SLA model was used to shape the donor bone for implant and the sterilized skull model was used to simulate the actual transplant surgery. The authors concluded that 3D printing helped in reducing surgical time and improving results for complex craniofacial surgeries (Fig. 5j–l). Sailer et al. (1998) used 3D printing (SLA) in multiple cases of craniofacial surgery including plagiocephaly, hypertelorism, Apert's syndrome, Crouzon's syndrome, Pfeiffer's syndrome, Treacher-Collins syndrome, and post-traumatic skull base and periorbital lesions, among others. The stereolithographic models of the various anatomies served diverse functions such

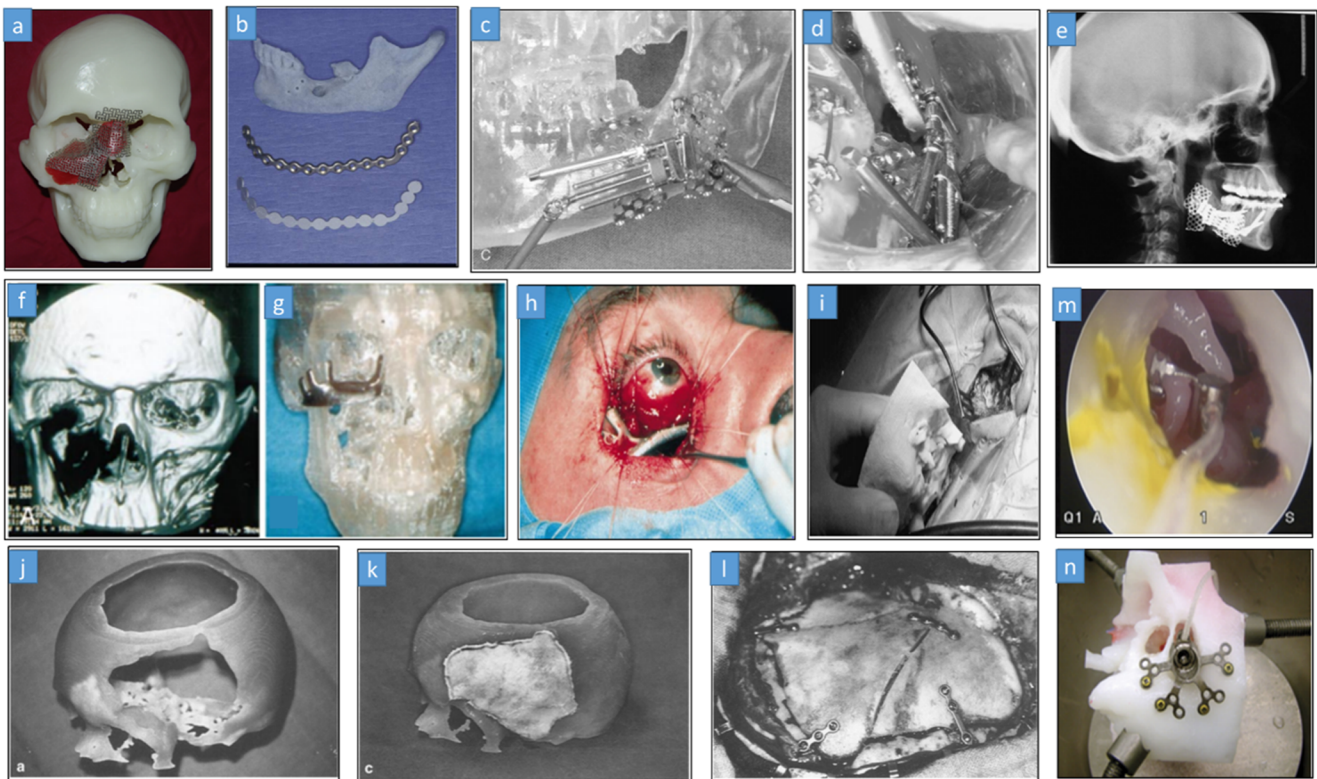


Fig. 5 3D printing applications in cranio-maxillo-facial surgery (a) Preshaping of titanium mesh implant on 3D printed model of a patient suffering from post-traumatic deformity (Cui et al. 2014) (Copyright © 2014 American Association of Oral and Maxillofacial Surgeons. Published by Elsevier Inc.) (b) SLA model of mandible and prebent reconstruction plate (Cunningham et al. 2005) (Copyright © 2005 American Association of Oral and Maxillofacial Surgeons. Published by Elsevier Inc.) (c–e) Distraction osteogenesis simulated on SLA model; intraoperative distractor position and radiographic image of the patient post operation (Robiony et al. 2008) (Copyright © 2008, 2008 by Mutaz B. Habal, MD.) (f–h) CT scan of right orbital bony defect; SLA model of

the same with custom fit titanium implant; intraoperative view of the implant (Holck et al. 1999) (Copyright © 1999 American Academy of Ophthalmology, Inc. Published by Elsevier Inc.) (i) 3D model of patient suffering from atresia of right ear used for surgical planning and its intraoperative view (Suzuki et al. 2005) (Copyright © 2005 Taylor & Francis) (j–l) 3D printed model of a cranial defect; shaping of the calvarial bone implant; the implant fit perfectly intraoperatively (Bill et al. 1995) (Copyright © 1995 Published by Elsevier Ltd.) (m–n) Surgeon training- posterior of the tympanic cavity and with a prosthesis carina screw (Bakhos et al. 2009) (Copyright © 2010, 2010 Otolaryngology)

as planning of cranial, skull base, orbital, or nasoethmoidal osteotomies, 3D-planning of orbital reassembly, assessment of periorbital deficiency, and planning of contouring and implant location. Satisfactory aesthetic and functional results were seen for all the cases. D'Urso et al. (1998) also used SLA in many similar cases. Two prominent cases included one patient with bicoronal craniosynostosis, a facial cleft, and hypertelorism; and the other patient with a very large right sided facial encephalocoele. The fabricated model was used to perform a surgical rehearsal by doing the exact osteotomy and reconstruction on the biomodels of both patients. These models helped predict possible intraoperative complications. The surgeons concluded that the ability to shape bone grafts intraoperatively using a biomodel template and to physically reconstruct the biomodels greatly improved the results of surgery. Later, similar use of 3D printed models specifically for hypertelorism surgical planning was demonstrated by Hidalgo et al. (2009). In another report, D'Urso et al. (2000) showed the use of 3D printing (SLA) to fabricate customized

cranioplastic implants for patients with craniotomy defects. The ideology and process route was similar to that of Bill et al. (1995), described previously. D'Urso et al. (2000) presented a 3D printing (inkjet and FDM) based cranial reconstruction approach for a patient with a large post-trauma defect in the left-frontal bone. The use of the 3D printed model, in addition to software simulation, allowed for a prosthesis creation that perfectly fit the defect and restored facial symmetry while reducing the operation time.

4.3.4 Orbital

Orbital reconstruction is a prominent craniofacial sub-section where 3D printing has shown a large presence in clinical simulation. Perry et al. (1998) published one of the first accounts in 1998, using stereolithography to produce models for patients suffering from various orbital deformities such as post-traumatic, fibrous dysplasia, radiation hypoplasia, high facial cleft, and partial Romberg syndrome. The models were crucial

in the planning of various procedures, including orbital volume restoration by resection of bone or grafting, and augmentation of a hypoplastic orbit using a lyo-cartilage graft to restore symmetry. For planning osteotomies of the orbital margins and the zygomatic complex, the models were useful for planned repositioning of the superior orbital rim and recontouring of the frontal bone. Satisfactory aesthetic and functional results were seen in all cases. Holck et al. (1999) published another report where 3D printed models were used for preoperative planning in two cases. For one patient, who was suffering from binocular vertical diplopia and globe compression due to displaced left orbital roof fracture, the SLA model was used to measure the dimensions of the displaced bone fragment along with its relationship to the anterior cranial fossa and the left frontal sinus. It was also used to plan and practice osteotomy. For a second patient suffering from binocular oblique diplopia and globe ptosis due to a previous excision surgery for cylindrical cell papilloma of the paranasal sinuses, the SLA model served as a template to fabricate a temporary custom-fit prosthesis to repair the defect of the orbital walls (Fig. 5f–h). The 3D printing-based procedure improved post-surgical outcomes with no complications. In a later report, Fan et al. (2007) demonstrated the application of SLA models for cases involving late reconstruction of complex orbital fractures, which can lead to aesthetic deformities as well as functional impairment, and are usually treated by pulling back herniated tissue into orbit and repairing the defect using an alloplastic implant. Reconstructing complex orbital fractures becomes more difficult if the bone healing has already occurred. Such late reconstruction procedures usually involve osteotomy, fractured bones, and globe reposition and fixation (Patel and Hoffmann 1998; Carr and Mathog 1997). The authors found that the 3D models in conjunction with software simulations helped in planning osteotomy, movement, reposition, and fixation of fractured bones and globe. Better pre-surgical planning resulted in improved surgical outcomes in all cases. Rohner et al. (2013) fabricated a 3D printed model for a patient requiring radical resection of the left orbit due to recurrence of an adenoid cystic carcinoma of the palate. The reconstruction was done with cranial bone grafts and a free latissimus dorsi flap. The model was used for planning of the resection, pre-bending of the reconstruction plate, and planning grafts from parietal bones apart from analyzing the anatomy. On a similar note, Park et al. (2015) used 3D printed skull-orbital anatomies to pre-mold synthetic scaffolds for optimal orbital cavity reconstruction. Postoperative complications were analyzed, and volumetric measurement of the orbital cavity showed insignificant volume differences between the damaged and reconstructed orbits. Moreover, successful reconstruction using this method was shown for patients who had lost more than 40% of their orbital wall in addition to soft tissue loss.

4.3.5 Ear

Surgery on a malformed ear demands a thorough anatomical understanding of the patient in addition to surgical experience. Tympanoplasty is especially difficult because of the anatomical complexity of the ear. Safe surgery to restore good hearing in cases such as atresia is difficult even after using CT imaging and virtual reconstruction. To address these challenges, Suzuki et al. (2005) demonstrated the use of selective laser sintering (SLS) to fabricate a 3D model for surgical simulation of a malformed ear. Abnormal structures of the middle ear such as the labyrinth, ossicles, and facial nerves were easily visualized in the models to aid in preoperative surgical planning (Fig. 5i). The authors showed similar surgical training work for ear surgeries. In another report, Bakhos et al. (2009) used stereolithography to prepare temporal bone models in which the surgical simulation of the posterior cavities, including a mastoidectomy followed by a trans-labyrinthine approach was possible. As a part of their surgical simulation exercise, two types of implantable middle ear prosthesis were introduced with satisfactory results (Fig. 5m–n). In a similar work, Longfield et al. (2015) showed the use of 3D printing for producing pediatric temporal bone for surgical training.

Cadaveric pediatric temporal bones are extremely rare, and no such training models existed before this. The fabricated temporal bone models were drilled for mastoid and facial recess as well as cochleostomy. Both models were assessed to be anatomically accurate with good mastoid pseudopneumatization and intact landmarks. The drilling efficacy for the models was found to be slightly softer than cadaveric temporal bones, and without the accompanied changes in density associated with the labyrinth, but was overall satisfactory. These models would greatly improve trainee learning experience, although at the current stage they cannot replace cadaveric models. Further work needs to address this limitation and this is discussed in the later sections.

4.4 Orthopedic surgery

This section discusses cases with applications of 3D printing in the general area of bone surgery, apart from the cranio-maxillo-facial cases discussed above. As a general orthopedic surgeon would usually see patients with fractures in different parts of the body, we found the same trend in the reports published. The reports in orthopedic surgery frequently involve work by a single author overlapping various parts of the body and are usually not limited to a particular anatomical location. Thus, we describe the review of these articles in their chronological order instead of dividing them into anatomy-based subsections.

Orthopedic surgery cases involving extensive primary injuries with multiple bone fragmentation or bone deformities pose significant challenges for the surgeon. In such cases,

custom implants and tools might be required to correctly shape the fixation plates and plan the surgical route, which requires thorough understanding of local shape variations and bone dimensions (McGurk et al. 1997). The revision of an orthopedic procedure is another example requiring a complex reconstructive process (John et al. 1995; Lachiewicz and Hussamy 1994; Kavanagh 1991). Changes in patient bone geometry, such as variation in local residue bone thickness after the last implant operation, can further complicate the case. It has been shown that joint replacement revisions have higher failure rates than primary cases (Kavanagh 1991; Bryan and Rand 1982). CT imaging data and 3D virtual reconstructions have been used to assist orthopedic surgical planning but they lack in providing the intuitive three-dimensional extent of bone defects, understanding of deformed bone anatomy, visualization of integration of bone fragments, or rehearsal of complex manipulations. 3D printed physical models from CT data can solve all the above problems, while also serving as a medium for explanation of the procedure to patients and obtaining informed consent. These physical models can be used, for example, to show the extent of tumor invasion into a bone, to study bone reassembly for cases of bone fragmentation, to build grooves to mark drilling procedures, and to test implants before the actual surgery.

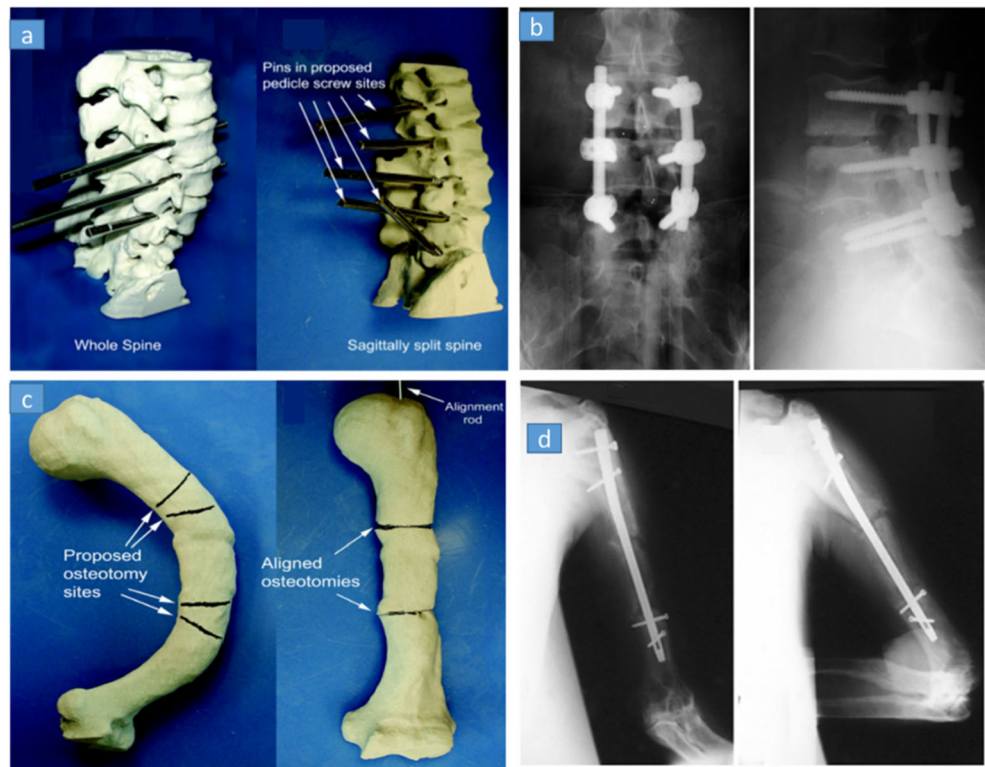
Potamianos et al. (2015) described the use of 3D printing (SLA) for a case involving a right shoulder injury with the possibility of a clavicle and scapula double fracture. Such a fracture, which would completely disconnect the bone between shoulder and trunk, would require extensive surgery with plate and screw stabilization and hence would need a confirmed diagnosis before proceeding. CT imaging data and 3D virtual reconstruction did not allow for a definitive diagnosis given the complexity of fracture lines in the case, so a 3D printed SLA model was fabricated to analyze the fracture. The model clearly showed that the fracture was not a floating shoulder type and that the clavicle sustained a complete transverse fracture, while the scapula remained partially attached. Once the diagnosis was confirmed, the patient was spared the unnecessary surgery.

In a later study, Brown et al. (2003) used 3D printing as a template guide to understand and correct several cases of severe acetabulum fractures, spine pathology, and fractures of the tibia, ankle, foot, pelvic ring, shoulder, arm, femur, knee, and wrist. 3D printed models of an unfractured hemipelvis were used to understand the anatomy, contour the reconstruction plates, and establish the drilling trajectories. Plaster models of the fractured hemipelvis were then used to test the implant positioning template prior to application in the patient. For cases of the spine, midline split spine models helped to elucidate the position of fracture fragments, the compromise of the spinal canal, and the complete pedicle visualization for pedicle screw placement including anatomic starting point,

screw trajectory, and length. 3D printed models with trajectories of pedicle screw placement were split into right and left halves and taken to the operating room with the patient for guidance. The models were also used to fix articular fractures, precisely position the plates, and direct osteotomies. For acetabular fractures, the contoured plate was positioned and locked with screws onto reduced fracture anatomy (Fig. 6). Similar works were published by Frame and Huntley (2012) and Guarino et al. (2007) showing applicability of rapid prototyping in forearm and spine-pelvis surgeries, respectively. In a different demonstration, Ahn et al. (2006) published 3D printing (polyjet) application in pre-surgical planning for distal tibia comminuted fracture and iliac wing fracture of the pelvis. In the first case, the physical model was used for proper implant selection and preforming of the implant to obtain satisfactory geometrical conformity to the contour of the physical model. For the second case, because the iliac wing of the pelvis had an excessive flexion, the pelvic reconstruction plate was chosen as the implant, as it could bend to conform to the bone shape. The implant fixation position, incision position, and its size were decided by using the 3D printed model. Satisfactory results and reduction in operation time were seen post-surgery in both situations. Hurson et al. (2007) published another report on the use of selective laser sintering (SLS) 3D printed models for the preoperative planning of acetabular fractures. The authors concluded that the models allowed better appreciation of the degree of anterior displacement of the fracture fragments and significantly reduced inter-observer variability during injury classification; additionally, SLS provided a full sized pelvic model in a relatively faster time (12 h). (Dhakshyani et al. 2010, 2012) published multiple papers on the use of rapid prototyping models for dysplastic hip orthopedic surgery. Dysplastic hip is a developmental hip disorder in which the acetabular roof is shallow, leading to early degeneration of the bone (Su et al. 2008; Mavčič et al. 2002; Umer et al. 2006). The authors showed that the FDM models allowed better surgical planning towards securing hip stability by proper implant size selection, bone grafting, femoral shortening, or proper consideration of high hip center and leg length discrepancy. The models also allowed for the selection of the best surgical route in advance.

Congenital scoliosis is a lateral curvature in the normally straight vertical line of the spine where early and aggressive deformity treatment can minimize risk to patient health. Posterior hemivertebra resection has proven to be an effective method for treatment of congenital scoliosis (Winter et al. 1984; Thompson and Marks 1995; Ruf and Harms 2002; Lazar and Hall 1999; Andrew and Piggott 1985). The surgical goal involves restoration of a straight spine and a physiological sagittal profile with the shortest fusion segment. Wu et al. (2011) showed that rapid prototyped models (such as FDM) can reduce the operation time, the risk

Fig. 6 3D printing applications in orthopedic surgery. **a–b** 3D printed model of lumbar spine of a fifty-year old woman with instability of L3-L4 and L4-L5 and with pins placed in proposed trajectories for pedicle screw insertions; anteroposterior and lateral radiographs of lumbar spine post-surgery. **c–d** 3D printed model of left humerus with proposed osteotomy sites and after alignment post simulation; internal and external rotation radiographs of left humerus post-surgery (Brown et al. 2003) (Copyright © 2003, by The Journal of Bone and Joint Surgery, Incorporated)



of pedicle screw misplacement, and its consequent complications in a number of cases of scoliosis treated with pedicle screw implants post hemivertebra resection. The authors concluded that although 3D CT (virtual reconstruction) allowed accurate identification of congenital spine anomalies, determination of many tangible skeletal parameters such as screw entry point, trajectory, and length, and pedicle diameter and thickness was possible only through 3D printed models.

In another approach, Debarre et al. (2012) assessed the feasibility of 3D printing (FDM) in assisting diagnosis of three cases: epiphyseal malunion, shoulder arthroplasty, and femoral trochleoplasty. In the first case, the FDM model helped in understanding the anatomy and in planning of the osteotomy lines. In the second case, the scapulohumeral 3D printed model enabled excellent estimation of available bone capital by manually comparing available bone volume to the intended implant and also allowed for practice of the glenosphere and screw positioning. For the third case, excessive relief of the proximal part of the trochlea was perfectly visible in the model, allowing its size to be quantified with precision. Moreover, are bony outgrowths on a normal bone such as “Spurs” and “double contours” were very accurately shown, facilitating trochleoplasty planning. In a similar setting, Starosolski et al. (2014) published a paper with 3D printing (FDM) application for a patient with a complex proximal femoral deformity from healing Perthes disease. The 3D printed model provided an understanding of the precise location and size of the femoral head and neck deformity as well as the degree of the hip

flexion when it came into contact with the acetabular rim. Studying the anatomy on the 3D model allowed for planning of the implant placement as well as rehearsal of the complete surgery on the model. The functionality was fully restored post-surgery.

4.5 Other

There are a few isolated reports published on 3D printing applications in organs areas not covered in the above sections. This section will discuss such special applications of 3D printing.

4.5.1 Lung

Bustamante et al. (2014) published a paper on using 3D printing (polyjet) technology for simulating bronchoscopic anatomy. Unfamiliarity with endoscopic bronchial anatomy is correlated with failure in achieving lung isolation, and the authors believe that these 3D bronchial anatomical models could bridge the knowledge gap. Also, uncommon and rare variants of the tracheobronchial tree can be replicated for training purposes. The authors fabricated two 3-dimensional models of the tracheobronchial tree, one with normal anatomy and the other with an early take off of the right apical bronchus. These models were then attached to mannequins and examined using flexible fiberoptic bronchoscope (FBB) and shown to be congruent to actual patient anatomy (Fig. 7a–c).

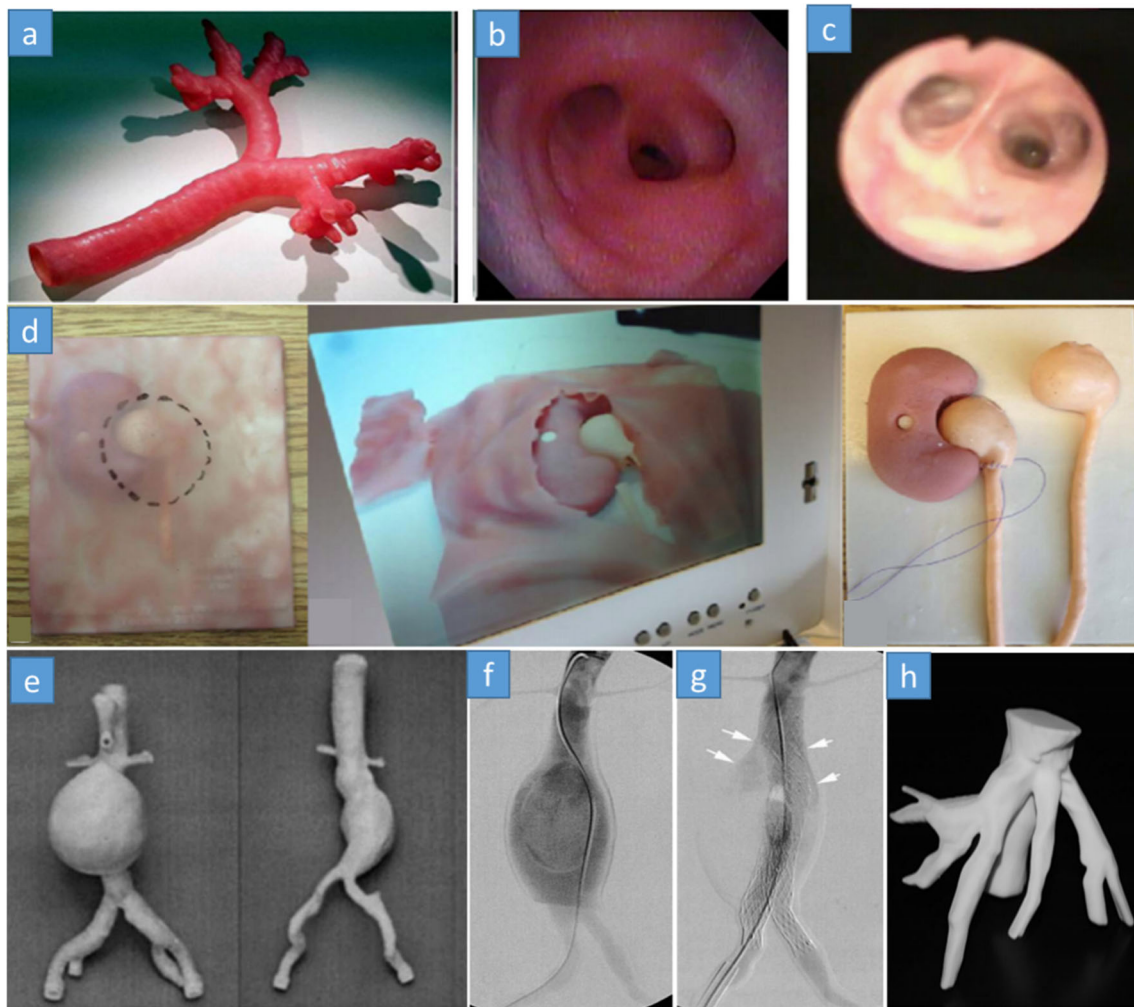


Fig. 7 3D printing applications in other areas. **a–c** 3D printed model of the tracheobronchial tree; fiberoptic view of bronchus intermedius for 3D model; fiberoptic view of bronchus intermedius in real anatomy (Bustamante et al. 2014) (Copyright © 2014 Elsevier Inc.) **(d)** pediatric pyeloplasty simulator with overlying peritoneum; dissection through the peritoneum and anastomosed ureter and renal pelvis, with replacement renal pelvis and ureter (Cheung et al. 2014) (Copyright © 2014

Association of Program Directors in Surgery. Published by Elsevier B.V.) **(e–g)** flexible silicone 3D models of human abdominal aortic aneurysms (AAA); digital subtraction angiogram of a replica perfused with contrast agent with a catheter; angiogram of a replica with a deployed stent (Berry et al. 2002) (Copyright © 2002, © SAGE Publications) **(h)** IVC and hepatic veins of a patient (Watson 2014). (Copyright © 2014 Published by Elsevier B.V.)

4.5.2 Renal

In another report, Cheung et al. (2014) demonstrated 3D printing application in surgical simulation of pediatric laparoscopic pyeloplasty. Due to smaller workspaces, finer sutures, and potentially more delicate tissues that required increased surgical dexterity, pediatric laparoscopy poses unique training challenges. A pediatric pyeloplasty model was created using 3D target organ models whose negative volume molds were 3D printed and cast with silicone rubber. For the simulator, the target organs included kidney, dilated renal pelvis, obstructed ureteropelvic junction, ureter, and overlying peritoneum, and the arrangement allowed for a traditional transmesenteric simulation. The organ shapes were

created by combining geometrical shapes, such as spheres and toroids, to approximate the organ. The models were scaled to the size of an approximately 10-month old (Fig. 7d).

4.5.3 Liver

Watson (2014) tested the use of 3D printing for the fabrication of physical hepatic models from CT or MRI data using selective laser sintering (SLS) for surgical resident education. The 3D models of the intrahepatic structures, including portal and hepatic veins, were printed. Hepatobiliary surgery, which is dependent on the understanding of individual, patient-specific variants of general anatomy, can greatly benefit from such models (Fig. 7h).

Table 1 3D printing method mapped to surgical area and their pros and cons

3D printing method	Cardiac surgery application areas	Neurosurgery application areas	Cranio-maxillo-facial application	Orthopaedic surgery application areas	Other application areas	Pros of method	Cons of method
1. SLS	<ul style="list-style-type: none"> - CHD cases 	<ul style="list-style-type: none"> - Skull base surgery 	<ul style="list-style-type: none"> - Unilateral maxillofacial deformities - Bilateral post-traumatic maxillofacial deformities - Tympanoplasty 	<ul style="list-style-type: none"> - Acetabular fractures 	<ul style="list-style-type: none"> - Hepatic 3D models - Flexible abdominal aortic aneurysms (AAA) with latex material 	<ul style="list-style-type: none"> - High accuracy - Large model size possible and large selection of materials - High strength allows drilling, other simulations - Moderate fabrication time for full sized models - Fabricated models allow device placements simulations (eg stent placement for flexible AAA models) 	<ul style="list-style-type: none"> - Very high cost - Finished models may have a powdery surface - Opaque models
2. SLA	<ul style="list-style-type: none"> - CHD cases - Pediatric cardiac transplant - Aortic stenosis - Cardiac tumor - Aneurysms 	<ul style="list-style-type: none"> - Brachyther apy - Skull base surgery - Cerebral aneurysms 	<ul style="list-style-type: none"> - Maxillofacial trauma - Congenital malformations - Severe skull defects and craniofacial surgery - Mandibular reconstruction - Dentofacial deformity - Orbital reconstruction 	<ul style="list-style-type: none"> - Shoulder injury 	<ul style="list-style-type: none"> - SLA mold for silicone rubber – abdominal aortic aneurysms 	<ul style="list-style-type: none"> - Very high accuracy - Large model size possible - Fabricated models allow device placement simulations (eg. Occluder device for aneurysms) - Implant/prosthesis design (eg. Distraction device for hemifacial microsomia) - Transparent models possible - Flexible models possible using rubber-like urethane (flexibility not perfect) - Models can be sterilized (USP class VI resin) 	<ul style="list-style-type: none"> - High cost - Moderate strength - Low speed
3. Inkjet (powder based 3D printing)	<ul style="list-style-type: none"> - CHD cases - Ventricular aneurysectomy and reshaping - Cardiac tumors - Transcatheter AVR and PPVI 	<ul style="list-style-type: none"> - Lesion near motor cortex - Surgical training involving skull drilling etc. 	<ul style="list-style-type: none"> - Cranial reconstruction 	<ul style="list-style-type: none"> - Fractures and deformities of tibia, ankle, foot, spine and acetabulum 	<ul style="list-style-type: none"> - 3D printed mold for silicon rubber – Pediatric laparoscopic pyeloplasty - Inkjet printing + lost wax technique: Arterial pathology models 	<ul style="list-style-type: none"> - Low cost - High speed - Multiple materials in a single model possible - Flexible models with starch as base material 	<ul style="list-style-type: none"> - Relatively lower accuracy - Relatively lower strength - Opaque models
4. FDM	<ul style="list-style-type: none"> - VSD - Aneurysm - Ulcerations - Prosthetic mitral valve perivalvular leak 	<ul style="list-style-type: none"> - FDM followed by silicone coating for hollow elastic models for cerebral aneurysm clipping simulation 	<ul style="list-style-type: none"> - Cranial reconstruction 	<ul style="list-style-type: none"> - Dysplastic hip - Scoliosis: restoration of straight spine - Epiphyseal malunion - Shoulder arthroplasty - Femoral trochleoplasty 	<ul style="list-style-type: none"> - Low cost - High accuracy - Catheter simulation possible on models - Implant selection based on models - Models can be sterilized for intraoperative use 	<ul style="list-style-type: none"> - Low speed - Removing support structures is time consuming - Opaque models 	
5. Polyjet	<ul style="list-style-type: none"> - Left atrial appendage closure - VSD in pediatric heart 	<ul style="list-style-type: none"> - NA 	<ul style="list-style-type: none"> - NA 	<ul style="list-style-type: none"> - Pelvic reconstruction - Distal tibia comminuted fracture 	<ul style="list-style-type: none"> - Bronchoscopic anatomy 	<ul style="list-style-type: none"> - Using rubber like material allows flexible heart models for simulation - Allows implant customization - High speed - High accuracy 	<ul style="list-style-type: none"> - Opaque models

CHD, Congenital heart disease; VSD, Ventricular septal defect; PPVI, Percutaneous pulmonary valve implantation; AVR, Aortic valve replacement; SLA, Stereolithography; FDM, Fused deposition modelling

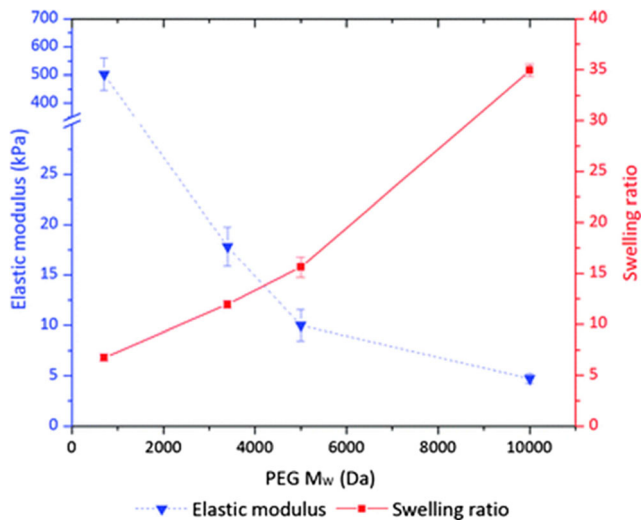


Fig. 8 The variation of elastic modulus and swelling of laser-polymerized PEGDA hydrogels with change in its molecular weight. The experiments were done with 20% PEGDA hydrogels and 0.5% photoinitiator concentration (Chan et al. 2010). (Copyright © 2010, Published by Royal Society of Chemistry)

4.5.4 Vascular (excluding cardiac and brain)

Chong et al. (1997) developed a simulator for endovascular repair of abdominal aortic aneurysms by using 3D printing (followed by silicone rubber molding) to fabricate transparent silicone rubber blocks with enclosed arterial lumens. This system was used to simulate the endovascular stent-graft deployment, a popular technique for repairing diseased vessels. The

model provided a good understanding of the aneurysm and its related vasculature, accurate dimensional measurements, and selection of correct device size. It also included renal, iliac, and femoral arteries with a temperature controlled blood-analog fluid perfused under simulated physiological flow conditions. The imaging system also permitted arteriography for determination of accurate stent-graft placement. Similar abdominal aortic models were fabricated by Berry et al. (2002) with SLS and flexible latex, and used for simulating stent placement (Fig. 7e–g). Knox et al. (2005) used 3D printing from CT angiographic data and a lost wax technique to create similar arterial pathology as discussed above. The lost wax technique uses 3D printed lumen anatomy to create a master mold followed by a wax lumen anatomy replica. This wax lumen is coated with silicone and then the wax is thermally and chemically removed, leaving behind a hollow, flexible silicone vessel. These vessels can allow surgeons to teach and practice dangerous interventional techniques. In a recent report, O'Reilly et al. (2015) used 3D printed anatomical models of the lower limb for anatomical teaching and femoral vessel access training in medicine. Using a combination of 3D printing, casting, and lost-wax technique, the authors fabricated an anatomically accurate lower limb model with hard bones, silicone muscles, and perfusable blood vessels, all held together by rare earth magnets. Vascular simulation is possible through application of pumps and artificial blood. These models allow creation of anatomically diverse samples which are very rare and permits their use for surgeon training (Table 1).

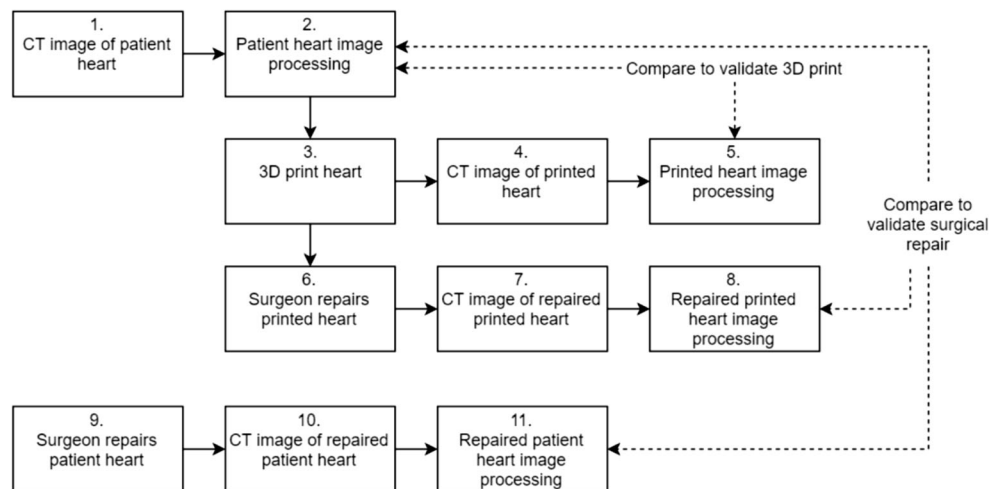


Fig. 9 Proposed process of 3D model fabrication, validation, and use for surgical planning, with an example from cardiology. (1) The patient heart is imaged using CT. (2) The CT image is processed through techniques such as segmentation, then converted into the appropriate STL file format for 3D printing. (3) The patient-specific model is 3D printed. (4) The printed model is imaged using CT. (5) The CT image of the print is processed, and then compared to the processed image of the patient heart in order to validate the 3D print. (6) Once assured that the printed model is identical to the patient heart, the surgeon operates on the printed model.

(7) The repaired model heart is CT imaged. (8) The CT image is processed, and then compared to the processed image of the patient heart in order to validate the surgeon's repair of the printed heart. (9) Once the surgeon has successfully operated on the printed heart, he will operate on the patient heart. (10) The repaired patient heart will be CT imaged. (11) The CT image of the repaired patient heart will be processed and then compared to the image of the repaired printed heart as well as the image of the patient heart prior to surgery in order to evaluate the surgical repair

5 Discussion and future perspective

This review highlights the applications of 3D printing in various areas of surgical simulation, including preoperative planning, intraoperative guidance, and surgeon training. 3D printed models have been used to replicate a broad spectrum of tissues, ranging from hard tissue structures such as the skull, spine, limbs, and ear bones, to soft tissue structures including the heart, lungs, liver, and vasculature. 3D printing in surgical assistance domain has seen a tremendous rise in the last two decades. However, despite significant progress, we find that the use of 3D printing to form soft tissue structures has been largely unexplored. Very few attempts have been made to capture the mechanical properties of soft tissue along with high resolution anatomical detail. Previous attempts utilized flexible polyurethane or silicone, but did not achieve the correct mechanical properties such as elastic modulus, and do not provide a true feel of the wet and soft biological tissue. Moreover, in the area of neurosurgery, a combination of hard and soft materials must be utilized to exactly simulate the skull as well as the underlying brain tissue. Such combinational approaches can also be very useful for other surgical areas. We have previously reported the stereolithographic printing of poly(ethylene) glycol-based hydrogels with control over mechanical properties (Fig. 8) (Chan et al. 2010). The wet nature of hydrogels can also add to the true feel of biological tissue in the printed model, and thus serve as an excellent material for soft tissue surgical simulations. The ability to 3D print hydrogel materials which mimic *in vivo* soft tissue properties has been widely utilized for tissue engineering applications, but these techniques have yet to be applied to the fabrication of anatomical models for surgical simulation (Farina et al. 2018; Moroni et al. 2018). An additional need is the ability to use materials that can be sutured, similar to real tissue. Figure 9 shows a proposed process of 3D model fabrication, validation, and use for surgical planning. If heart defects, for example, can be recapitulated via printing, then the surgeons can fix the defects via surgical suturing. The surgical fix can be imaged again and the performance of the surgeons can be quantified precisely and surgeons can improve their skills by repeating the procedure multiple times. We believe that with future developments in these printed materials, the next generation of surgical simulations will possess an added realism which will significantly improve surgical training and preoperative planning, resulting in increased success rates in surgical operations. Furthermore, in March 2018, Materialise became the first company to receive FDA clearance for 3D printed anatomical model software intended for diagnostic use. As stated by Materialise CEO, Wilfried Vancaeren, the FDA approval of Materialise Mimics software will “support the adoption of 3D planning and printing in U.S. hospitals and the creation of point-of-care 3D printing facilities”.

Considering recent advances in 3D printing softwares and model materials together with the FDA’s approval of this technology for diagnostic use, the applications of 3D printed anatomical models will continue to expand and further improve healthcare.

References

- P. Abdel-Sayed, L. Von Segesser, in *Adv. Appl. Rapid Prototyp. Technol. Mod. Eng.*. Rapid prototyping for training purposes in cardiovascular surgery (2011)
- P. Abdel-Sayed, M. Kalejs, L.K. von Segesser, A new training set-up for trans-apical aortic valve replacement. *Interact. Cardiovasc. Thorac. Surg.* **8**, 599–601 (2009)
- N. Adolphs, W. Liu, E. Keeve, B. Hoffmeister, Craniomaxillofacial surgery planning based on 3D models derived from Cone-Beam CT data. *Comput. Aided Surg.* **18**(5–6), 101–108 (2013)
- D.-G. Ahn, J.-Y. Lee, D.-Y. Yang, Rapid prototyping and reverse engineering application for orthopedic surgery planning. *J. Mech. Sci. Technol.* **20**(1), 19–28 (2006)
- M. Akaike et al., Simulation-based medical education in clinical skills laboratory. *J. Med. Invest.* **59**(1, 2), 28–35 (2012)
- O. Al-Mefty, J.L. Fox, A. Rifai, R.R. Smith, A combined infratemporal and posterior fossa approach for the removal of giant glomus tumors and chondrosarcomas. *Surg. Neurol.* **28**(6), 423–431 (Dec. 1987)
- T. Andrew and H. Piggott, Growth arrest for progressive scoliosis. Combined anterior and posterior fusion of the convexity. *J. Bone Jt. Surg.* ..., (1985)
- E. Angeli, D. Pacini, S. Martin-Suarez, A. Dell’Amore, R. Fattori, R. Di Bartolomeo, Stent repair of aortic perianastomotic leak after aortic arch and descending aorta replacement. *Ital. Heart J. Off. J. Ital. Fed. Cardiol.* **5**(12), 951–953 (Dec. 2004)
- D. Bakhos, S. Velut, A. Robier, M. Al Zahrani, E. Lescanne, Three-dimensional modeling of the temporal bone for surgical training. *Otol. Neurotol. Off. Publ. Am. Otol. Soc. Am. Neurotol. Soc. Eur. Acad. Otol. Neurotol.*, 328–334 (2009)
- E. Berry et al., Preliminary experience with medical applications of rapid prototyping by selective laser sintering. *Med. Eng. Phys.* **19**(1), 90–96 (1997)
- E. Berry, A. Marsden, K.W. Dalgarno, D. Kessel, D.J. Scott, Flexible tubular replicas of abdominal aortic aneurysms. *Proc. Inst. Mech. Eng. H J. Eng. Med.* **216**(3), 211–214 (2002)
- Bertalanffy, The dorsolateral, suboccipital, transcondylar approach to the lower clivus and anterior portion of the craniocervical junction. *Neurosurgery* **29**(6), 815–821 (1991)
- J.S. Bill et al., Stereolithography in oral and maxillofacial operation planning. *Int. J. Oral Maxillofac. Surg.* **24**(1), 98–103 (Feb. 1995)
- G.A. Brown, K. Firoozbakhsh, T. a DeCoster, J.R. Reyna, M. Moneim, Rapid prototyping: the future of trauma surgery? *J. Bone Joint Surg. Am.* **85**(A Suppl), 49–55 (2003)
- R. Bryan, J. Rand, *Revision total knee arthroplasty* (Clin. Orthop, 1982)
- S. Bustamante, S. Bose, P. Bishop, R. Klatte, F. Norris, Novel application of rapid prototyping for simulation of bronchoscopic anatomy. *J. Cardiothorac. Vasc. Anesth.* **28**(4), 1134–1137 (2014)
- R.M. Carr, R.H. Mathog, Early and delayed repair of orbitozygomatic complex fractures. *J. Oral Maxillofac. Surg.* **55**(3), 253–258 (Mar. 1997)
- V. Chan, P. Zorlutuna, J.H. Jeong, H. Kong, R. Bashir, Three-dimensional photopatterning of hydrogels using stereolithography for long-term cell encapsulation. *Lab. Chip* **10**(16), 2062–2070 (Aug. 2010)
- C.L. Cheung, T. Looi, T.S. Lendvay, J.M. Drake, W.a. Farhat, Use of 3-dimensional printing technology and silicone modeling in surgical

- simulation: Development and face validation in pediatric laparoscopic pyeloplasty. *J. Surg. Educ.* **71**(5), 762–767 (2014)
- C. K. Chong, J. Brennan, T. V. How, R. Edwards, G. L. Gilling-Smith, and P. L. Harris, “A prototype simulator for endovascular repair of abdominal aortic aneurysms,” *Eur. J. Vasc. Endovasc. Surg. Off. J. Eur. Soc. Vasc. Surg.*, vol. 13, no. 3, pp. 330–333, 1997.
- A. Cohen, A. Laviv, P. Berman, R. Nashef, J. Abu-Tair, Mandibular reconstruction using stereolithographic 3-dimensional printing modeling technology. *Oral Surg. Oral Med. Oral Pathol. Oral Radiol. Endodontology* **108**(5), 661–666 (2009)
- J.J. Collins, S.F. Aranki, Management of mild aortic stenosis during coronary artery bypass graft surgery. *J. Card. Surg.* **9**(s2), 145–147 (Mar. 1994)
- J.P. Costello et al., Utilizing three-dimensional printing technology to assess the feasibility of high-fidelity synthetic ventricular septal defect models for simulation in medical education. *World J. Pediatr. Congenit. Heart Surg.* **5**(3), 421–426 (2014)
- J.P. Costello et al., Incorporating three-dimensional printing into a simulation-based congenital heart disease and critical care training curriculum for resident physicians. *Congenit Heart Dis* **10**(2), 185–190 (2015)
- J. Cui, L. Chen, X. Guan, L. Ye, H. Wang, L. Liu, Surgical planning, three-dimensional model surgery and preshaped implants in treatment of bilateral craniomaxillofacial post-traumatic deformities. *J. Oral Maxillofac. Surg.* **72**(6), 1138.e1–1138.e14 (2014)
- L.L. Cunningham, M.J. Madsen, G. Peterson, Stereolithographic modeling technology applied to tumor resection. *J. Oral Maxillofac. Surg.* **63**(6), 873–878 (2005)
- P.S. D’Urso et al., Stereolithographic (SL) biomodelling in craniofacial surgery. *Br. J. Plast. Surg.* **51**(7), 522–530 (Oct. 1998)
- P.S. D’Urso et al., Custom cranioplasty using stereolithography and acrylic. *Br. J. Plast. Surg.* **53**(3), 200–204 (Apr. 2000)
- E. Debarre, P. Hivart, D. Baranski, P. Déprez, Speedy skeletal prototype production to help diagnosis in orthopaedic and trauma surgery. *Methodology and examples of clinical applications. Orthop. Traumatol. Surg. Res.* **98**(5), 597–602 (2012)
- R. Dhakshyani, Y. Nukman, N.A.A. Osman, A.M. Merican, J. George, Rapid prototyping medical models for dysplastic hip orthopaedic surgery. *Proc. Inst. Mech. Eng. Part B J. Eng. Manuf.* **224**(5), 769–776 (2010)
- R. Dhakshyani, Y. Nukman, N.A. Abu Osman, Rapid prototyping models for dysplastic hip surgeries in Malaysia. *Eur. J. Orthop. Surg. Traumatol.* **22**(1), 41–46 (2012)
- B.O. Erbaro et al., Rapid prototyping of three-dimensional biomodels as an adjuvant in the surgical planning for intracranial aneurysms. *Acta Cirúrgica Bras. Soc. Bras. Para Desenvolv. Pesqui. Em Cir.* **28**(11), 756–761 (2013)
- X. Fan, H. Zhou, M. Lin, Y. Fu, J. Li, Late reconstruction of the complex orbital fractures with computer-aided design and computer-aided manufacturing technique. *J. Craniofac. Surg.* **18**(3), 665–673 (2007)
- M. Farina, J.F. Alexander, U. Thekkedath, M. Ferrari, A. Grattoni, Cell encapsulation: Overcoming barriers in cell transplantation in diabetes and beyond. *Adv. Drug Deliv. Rev.* (2018)
- S.F. Fighali et al., Early and late mortality of patients undergoing aortic valve replacement after previous coronary artery bypass graft surgery. *Circulation* **92**(9), 163–168 (Nov. 1995)
- U. Fisch, The infratemporal approach to glomus jugulare tumors. *Neurochirurgie.* **31**(5), 367–376 (Jan. 1985)
- D.H. Frakes, M.J.T. Smith, J. Parks, S. Sharma, S.M. Fogel, A.P. Yoganathan, New techniques for the reconstruction of complex vascular anatomies from MRI images. *J. Cardiovasc. Magn. Reson. Off. J. Soc. Cardiovasc. Magn. Reson.* **7**(2), 425–432 (2005)
- M. Frame, J.S. Huntley, Rapid prototyping in orthopaedic surgery: a user’s guide. *ScientificWorldJournal* **2012**, 838575 (2012)
- K. Futami, M. Nakada, M. Iwato, D. Kita, T. Miyamori, J. Yamashita, Simulation of clipping position for cerebral aneurysms using three-dimensional computed tomography angiography. *Neurol. Med. Chir. (Tokyo)* **44**(1), 6–13 (Mar. 2004)
- J. Gateno, M.E. Allen, J.F. Teichgraber, M.L. Messersmith, An *in vitro* study of the accuracy of a new protocol for planning distraction osteogenesis of the mandible. *J. Oral Maxillofac. Surg. Off. J. Am. Assoc. Oral Maxillofac. Surg.* **58**(9), 985–990; discussion 990–1 (2000)
- J. Geerts et al., Functional magnetic resonance imaging for preoperative localisation of eloquent brain areas relative to brain tumours: clinical implementation in a regional hospital. *JBR-BTR Organe Société R. Belge Radiol. SRBR Orgaan Van K. Belg. Ver. Voor Radiol. KBVR* **90**(4), 258–263 (Jan. 2007)
- K.K. Gnanalingham, V. Apostolopoulos, S. Barazi, K. O’Neill, The impact of the international subarachnoid aneurysm trial (ISAT) on the management of aneurysmal subarachnoid haemorrhage in a neurosurgical unit in the UK. *Clin. Neurol. Neurosurg.* **108**(2), 117–123 (Feb. 2006)
- G.F. Greil et al., Stereolithographic reproduction of complex cardiac morphology based on high spatial resolution imaging. *Clin. Res. Cardiol.* **96**, 176–185 (2007)
- J. Guarino, S. Tennyson, G. McCain, L. Bond, K. Shea, H. King, Rapid prototyping technology for surgeries of the pediatric spine and pelvis: benefits analysis. *J. Pediatr. Orthop.* **27**(8), 955–960 (2007)
- H.K. Hahn, W.S. Millar, O. Klinghammer, M.S. Durkin, P.K. Tulipano, H.-O. Peitgen, A reliable and efficient method for cerebral ventricular volumetry in pediatric neuroimaging. *Methods Arch.* **43**(4), 376–382 (2004)
- H.M. Hidalgo, G.W. Romo, R.T.R. Estolano, Stereolithography: a method for planning the surgical correction of the hypertelorism. *J. Craniofac. Surg.*, vol. 5, 20 (2009)
- J. Hirsch et al., An integrated functional magnetic resonance imaging procedure for preoperative mapping of cortical areas associated with tactile, motor, language, and visual functions. *Neurosurgery* **47**(3), 711–722 (2000)
- J.I. Hoffman, S. Kaplan, The incidence of congenital heart disease. *J. Am. Coll. Cardiol.* **39**(12), 1890–1900 (Jun. 2002)
- D.E. Holck, E.M. Boyd, J. Ng, R.O. Mauffray, Benefits of stereolithography in orbital reconstruction. *Ophthalmology* **106**(6), 1214–1218 (1999)
- C. Hurson, B.O.’D. a Tansey, P. Nicholson, J. Rice, J. McElwain, Rapid prototyping in the assessment, classification and preoperative planning of acetabular fractures. *Injury* **38**(10), 1158–1162 (2007)
- S. Jacobs, R. Grunert, F.W. Mohr, V. Falk, 3D-Imaging of cardiac structures using 3D heart models for planning in heart surgery: a preliminary study. *Interact. Cardiovasc. Thorac. Surg.* **7**(1), 6–9 (2008)
- A.D. Jatene, Left ventricular aneurysmectomy. Resection or reconstruction. *J. Thorac. Cardiovasc. Surg.* **89**(3), 321–331 (Mar. 1985)
- J.F. John, R.E. Talbert, J.K. Taylor, W.L. Bargar, Use of acetabular models in planning complex acetabular reconstructions. *J. Arthroplasty* **10**(5), 661–666 (Oct. 1995)
- M. Kalejs, L.K. von Segesser, Rapid prototyping of compliant human aortic roots for assessment of valved stents. *Interact. Cardiovasc. Thorac. Surg.* **8**, 182–186 (2009)
- T. Kaminaga, T. Takeshita, I. Kimura, Role of magnetic resonance imaging for evaluation of tumors in the cardiac region. *Eur. Radiol.*, vol. 13 Suppl 6, L1–L10 (Dec. 2003)
- B. Kavanagh, Cemented revision hip arthroplasty: results, *Jt. Replace. Arthroplasty N. Y. Etc Churchill ... 1991 Paperpile.*
- C.J. Kellenberger, S.-J. Yoo, E.R.V. Büchel, Cardiovascular MR imaging in neonates and infants with congenital heart disease. *Radiogr. Rev. Publ. Radiol. Soc. N. Am. Inc* **27**(1), 5–18 (2007)
- C. Kermer, a. Lindner, I. Friede, a. Wagner, W. Millesi, Preoperative stereolithographic model planning for primary reconstruction in

- craniomaxillofacial trauma surgery. *J. Craniomaxillofac. Surg.* **26**(3), 136–139 (1998)
- J. Kettenbach et al., Computer-based imaging and interventional MRI: applications for neurosurgery. *Comput. Med. Imaging Graph.* **23**(5), 245–258 (1999)
- M.S. Kim, A.R. Hansgen, O. Wink, R.A. Quaife, J.D. Carroll, Rapid prototyping: a new tool in understanding and treating structural heart disease. *Circulation* **117**(18), 2388–2394 (2008)
- T. Kimura et al., Simulation of and training for cerebral aneurysm clipping with 3-dimensional models. *Neurosurgery* **65**(4), 719–726 (2009)
- K. Knox, C.W. Kerber, S. a Singel, M.J. Bailey, S.G. Imbesi, Rapid prototyping to create vascular replicas from CT scan data: making tools to teach, rehearse, and choose treatment strategies. *Catheter. Cardiovasc. Interv. Off. J. Soc. Card. Angiogr. Interv.* **65**(1), 47–53 (2005)
- M. Kozakiewicz et al., Clinical application of 3D pre-bent titanium implants for orbital floor fractures. *J. Cranio-Maxillofac. Surg.* **37**(4), 229–234 (2009)
- J.P. Kruth, Material in-process manufacturing by rapid prototyping techniques. *CIRP Ann. - Manuf. Technol.* **40**(2), 603–614 (1991)
- P. Lachiewicz and O. Hussamy, Revision of the acetabulum without cement with use of the Harris-Galante porous-coated implant. Two to eight-year results. *J. Bone Jt. Surg.*, (1994)
- R. Lazar and J. Hall, Simultaneous anterior and posterior hemivertebra excision. *Clin. Orthop.*, (1999)
- G.M. Lemole, P.P. Banerjee, C. Luciano, S. Neckrysh, F.T. Charbel, Virtual reality in neurosurgical education. *Neurosurgery* **61**(1), 142–149 (2007)
- E.A. Longfield, T.M. Brickman, A. Jeyakumar, 3D printed pediatric temporal bone: a novel training model. *Otol Neurotol*, 793–795 (2015)
- E. Maravelakis, K. David, A. Antoniadis, A. Manios, N. Bilalis, Y. Papaharilaou, Reverse engineering techniques for cranioplasty: a case study. *J. Med. Eng. Technol.* **32**(2), 115–121 (2008)
- T. Mashiko et al., Development of three-dimensional hollow elastic model for cerebral aneurysm clipping simulation enabling rapid and low cost prototyping. *World Neurosurg* **83**(3), 351–361 (2015)
- B. Mavčič, B. Pompe, and V. Antolič, Mathematical estimation of stress distribution in normal and dysplastic human hips, J. (2002)
- M. McGurk, A.A. Amis, P. Potamianos, N.M. Goodger, Rapid prototyping techniques for anatomical modelling in medicine. *Ann. R. Coll. Surg. Engl.* **79**(3), 169–174 (May 1997)
- S. Mohammadi et al., Reoperation for false aneurysm of the ascending aorta after its prosthetic replacement: surgical strategy. *Ann. Thorac. Surg.* **79**(1), 147–152; discussion 152 (Jan. 2005)
- K. Mori, T. Yamamoto, K. Oyama, H. Ueno, Y. Nakao, K. Honma, Modified three-dimensional skull base model with artificial dura mater, cranial nerves, and venous sinuses for training in skull base surgery: technical note. *Neurol. Med. Chir. (Tokyo)* **48**(12), 582–587; discussion 587–588 (2008)
- L. Moroni et al., Biofabrication strategies for 3D in vitro models and regenerative medicine, *Nature Reviews Materials.* **3**(5), 21–37, (2018)
- S. Mottl-Link et al., Physical models aiding in complex congenital heart surgery. *Ann. Thorac. Surg.* **86**(1), 273–277 (2008)
- B. Mueller, D. Kochan, Laminated object manufacturing for rapid tooling and patternmaking in foundry industry. *Comput. Ind.* **39**(1), 47–53 (1999)
- A. Müller, K.G. Krishnan, E. Uhl, G. Mast, The application of rapid prototyping techniques in cranial reconstruction and preoperative planning in neurosurgery. *J. Craniofac. Surg.* **14**, 899–914 (2003)
- M.C. Murphy et al., Surgical treatment of cardiac tumors: A 25-year experience☆. *Ann. Thorac. Surg.* **49**(4), 612–618 (Apr. 1990)
- S.F. Mustafa, P.L. Evans, A. Bocca, D.W. Patton, A.W. Sugar, P.W. Baxter, Customized titanium reconstruction of post-traumatic orbital wall defects: a review of 22 cases. *Int. J. Oral Maxillofac. Surg.* **40**(12), 1357–1362 (2011)
- E.M. Ngan et al., The rapid prototyping of anatomic models in pulmonary atresia. *J. Thorac. Cardiovasc. Surg.* **132**(2), 264–269 (2006)
- A.M. Noecker et al., Development of patient-specific three-dimensional pediatric cardiac models. *ASAIO J.* **52**(3), 349–353 (2006)
- M.K. O'Reilly et al., Fabrication and assessment of 3D printed anatomical models of the lower limb for anatomical teaching and femoral vessel access training in medicine. *Anat. Sci. Educ.* **00**(2010), 1–9 (2015)
- J.A. Odell, C.J. Mullany, H.V. Schaff, T.A. Orszulak, R.C. Daly, J.J. Morris, Aortic valve replacement after previous coronary artery bypass grafting. *Ann. Thorac. Surg.* **62**(5), 1424–1430 (Nov. 1996)
- M. Oishi, M. Fukuda, N. Yajima, and K. Yoshida, Interactive presurgical simulation applying advanced 3D imaging and modeling techniques for skull base and deep tumors: Clinical article, *J. Of.* (2013).
- M. Oliveira et al., 3-D biomodelling technology for maxillofacial reconstruction. *Mater. Sci. Eng. C* **28**(8), 1347–1351 (2008)
- L.J. Olivieri, A. Krieger, Y.-H. Loke, D.S. Nath, P.C.W. Kim, C.A. Sable, Three-dimensional printing of intracardiac defects from three-dimensional echocardiographic images: feasibility and relative accuracy. *J. Am. Soc. Echocardiogr.* **28**(4), 392–397 (2015)
- J.M. Otton et al., Left atrial appendage closure guided by personalized 3d-printed cardiac reconstruction. *JACC Cardiovasc. Interv.* **8**(7), 1004–1006 (2015)
- P. Ou, D.S. Celermajer, G. Calcagni, F. Brunelle, D. Bonnet, D. Sidi, Three-dimensional CT scanning: a new diagnostic modality in congenital heart disease. *Heart* **93**(8), 908–913 (2007)
- S.W. Park, J.W. Choi, K.S. Koh, T.S. Oh, Mirror-imaged rapid prototype skull model and pre-molded synthetic scaffold to achieve optimal orbital cavity reconstruction. *J. Oral Maxillofac. Surg. Off. J. Am. Assoc. Oral Maxillofac. Surg.*, 1540–1553 (2015)
- J.Y. Park, G. Gao, J. Jang, D.-W. Cho, 3D printed structures for delivery of biomolecules and cells: tissue repair and regeneration. *J. Mater. Chem. B* **4**(47), 7521–7539 (2016)
- B.C. Patel, J. Hoffmann, Management of complex orbital fractures. *Facial Plast. Surg. FPS* **14**(1), 83–104 (Jan. 1998)
- M. Perry, P. Banks, R. Richards, E.P. Friedman, P. Shaw, The use of computer-generated three-dimensional models in orbital reconstruction. *Br. J. Oral Maxillofac. Surg.* **36**(4), 275–284 (1998)
- P. Potamianos, A.A. Amis, A.J. Forester, M. McGurk, M. Bircher, Rapid prototyping for orthopaedic surgery. *Proc Inst Mech Eng Part H* **212**, 383–393 (2015)
- M. Poulsen, C. Lindsay, T. Sullivan, P. D'Urso, Stereolithographic modelling as an aid to orbital brachytherapy. *Int. J. Radiat. Oncol. Biol. Phys.* **44**(3), 731–735 (1999)
- M.D. Reller, M.J. Strickland, T. Riehle-Colarusso, W.T. Mahle, A. Correa, Prevalence of congenital heart defects in metropolitan Atlanta, 1998–2005. *J. Pediatr.* **153**(6), 807–813 (Dec. 2008)
- F. Rengier et al., 3D printing based on imaging data: review of medical applications. *Int. J. Comput. Assist. Radiol. Surg.* **5**(4), 335–341 (2010)
- M. Robiony et al., Accuracy of virtual reality and stereolithographic models in maxillo-facial surgical planning. *J. Craniofac. Surg.* **19**(2), 482–489 (2008)
- D. Rohner, R. Guijarro-Martínez, P. Bucher, B. Hammer, Importance of patient-specific intraoperative guides in complex maxillofacial reconstruction. *J. Cranio-Maxillofac. Surg.* **41**(5), 382–390 (2013)
- M. Ruf and J. Harms, Hemivertebra resection by a posterior approach: innovative operative technique and first results. *Spine*, (2002)
- H.F. Sailer, P.E. Haers, C.P. Zollikofer, T. Warnke, F.R. Carls, P. Stucki, The value of stereolithographic models for preoperative diagnosis of craniofacial deformities and planning of surgical corrections. *Int. J. Oral Maxillofac. Surg.* **27**(5), 327–333 (1998)

- E.K. Sannomiya, J.V.L. Silva, A.A. Brito, D.M. Saez, F. Angelieri, G. da Silva Dalben, Surgical planning for resection of an ameloblastoma and reconstruction of the mandible using a selective laser sintering 3D biomodel. *Oral Surg. Oral Med. Oral Pathol. Oral Radiol. Endod* **106**, 36–40 (2008)
- C. Santler, H. Karcher, C. Ruda, Indications and limitations of three-dimensional models in cranio-maxillofacial surgery. *J. Craniomaxillofac. Surg.* **26**(1), 11–16 (1998)
- R.M. Satava, Accomplishments and challenges of surgical simulation. *Surg. Endosc.* **15**(3), 232–241 (Mar. 2001)
- S. Schievano et al., Percutaneous pulmonary valve implantation based on rapid prototyping of right ventricular outflow tract and pulmonary trunk from MR data. *Radiology* **242**(2), 490–497 (2007)
- D. Schmauss et al., Three-dimensional printing of models for preoperative planning and simulation of transcatheter valve replacement. *Ann. Thorac. Surg.* **93**(2), e31–e33 (2012)
- D. Schmauss, N. Gerber, R. Sodian, Three-dimensional printing of models for surgical planning in patients with primary cardiac tumors. *J. Thorac Cardiovasc Surg* **145**(5), 1407–1408 (2013)
- I. Shiraiishi, M. Yamagishi, K. Hamaoka, M. Fukuzawa, T. Yagihara, Simulative operation on congenital heart disease using rubber-like urethane stereolithographic biomodels based on 3D datasets of multislice computed tomography. *Eur. J. Cardio-Thorac. Surg. Off. J. Eur. Assoc. Cardio-Thorac. Surg.* **37**(2), 302–306 (2010)
- D.P. Sinn, J.E. Cillo, B. a Miles, Stereolithography for craniofacial surgery. *J. Craniofac. Surg.* **17**(5), 869–875 (2006)
- R. Sodian et al., Stereolithographic models for surgical planning in congenital heart surgery. *Ann. Thorac. Surg.* **83**, 1854–1857 (2007)
- R. Sodian et al., Pediatric cardiac transplantation: Three-dimensional printing of anatomic models for surgical planning of heart transplantation in patients with univentricular heart. *J. Thorac. Cardiovasc. Surg.* **136**(4), 1098–1099 (2008a)
- R. Sodian et al., Three-dimensional printing creates models for surgical planning of aortic valve replacement after previous coronary bypass grafting. *Ann. Thorac. Surg.* **85**(6), 2105–2108 (2008b)
- R. Sodian et al., 3-dimensional printing of models to create custom-made devices for coil embolization of an anastomotic leak after aortic arch replacement. *Ann. Thorac. Surg.* **88**(3), 974–978 (2009)
- P.J. Spevak, P.T. Johnson, E.K. Fishman, Surgically corrected congenital heart disease: utility of 64-MDCT. *AJR Am. J. Roentgenol.* **191**(3), 854–861 (2008)
- B.S. Spottiswoode et al., Preoperative three-dimensional model creation of magnetic resonance brain images as a tool to assist neurosurgical planning. *Stereotact. Funct. Neurosurg.* **91**(3), 162–169 (2013)
- A.T. Stadie et al., Virtual reality system for planning minimally invasive neurosurgery. Technical note. *J. Neurosurg.* **108**(2), 382–394 (Feb. 2008)
- Z.A. Starosolski, J.H. Kan, S.D. Rosenfeld, R. Krishnamurthy, A. Annappagada, Application of 3-D printing (rapid prototyping) for creating physical models of pediatric orthopedic disorders. *Pediatr. Radiol.* **44**(2), 216–221 (2014)
- Y. Su, M. Wang, and W. Chang, Slotted acetabular augmentation in the treatment of painful residual dysplastic hips in adolescents and young adults. *J. Formos. Med. ...*, (2008)
- M. Suzuki, Y. Ogawa, A. Hagiwara, H. Yamaguchi, H. Ono, Rapidly prototyped temporal bone model for otological education. *ORL J. Oto-Rhino-Laryngol. Its Relat. Spec.* **66**(2), 62–64 (2004a)
- M. Suzuki, Y. Ogawa, A. Kawano, A. Hagiwara, H. Yamaguchi, H. Ono, Rapid prototyping of temporal bone for surgical training and medical education. *Acta Otolaryngol. (Stockh.)* **124**(4), 400–402 (2004b)
- M. Suzuki, A. Hagiwara, S. Kawaguchi, H. Ono, Application of a rapid-prototyped temporal bone model for surgical planning. *Acta Otolaryngol. (Stockh.)* **125**(1), 29–32 (Jan. 2005)
- A. Thompson and D. Marks, Long-term results of combined anterior and posterior convex epiphysiodesis for congenital scoliosis due to hemivertebrae. *Spine*, (1995)
- J.W.M. Tyl, L.E.C.M. Blank, L. Koornneef, Brachytherapy in orbital tumors. *Ophthalmology* **104**(9), 1475–1479 (Sep. 1997)
- M. Umer, A. Thambyah, W. Tan, and S. De, Acetabular morphometry for determining hip dysplasia in the Singaporean population. *J. Orthop. ...*, (2006)
- P. S. D. Urso et al., A technical note, (1999).
- I. Valverde et al., Three-dimensional printed models for surgical planning of complex congenital heart defects: an international multicentre study. *Eur. J. Cardio-Thorac. Surg. Off. J. Eur. Assoc. Cardio-Thorac. Surg.* **52**(6), 1139–1148 (Dec. 2017)
- M. Vranicar, W. Gregory, W.I. Douglas, P. Di Sessa, T.G. Di Sessa, The use of stereolithographic hand held models for evaluation of congenital anomalies of the great arteries. *Stud. Health Technol. Inform.* **132**, 538–543 (Jan. 2008)
- V. Waran et al., Injecting realism in surgical training—initial simulation experience with custom 3d models. *J. Surg. Educ.* **71**(2), 193–197 (2014a)
- V. Waran, V. Narayanan, R. Karuppiyah, S.L.F. Owen, T. Aziz, Utility of multimaterial 3D printers in creating models with pathological entities to enhance the training experience of neurosurgeons. *J. Neurosurg.* **120**(2), 489–492 (2014b)
- V. Waran et al., Neurosurgical endoscopic training via a realistic 3-dimensional model with pathology. *Simul. Healthc. J. Soc. Simul. Healthc.* **10**(1), 43–48 (2015)
- R.A. Watson, A Low-Cost Surgical Application of Additive Fabrication. *J. Surg. Educ.* **71**(1), 14–17 (2014)
- J. Winder, R. Bibb, Medical rapid prototyping technologies: state of the art and current limitations for application in oral and maxillofacial surgery. *J. Oral Maxillofac. Surg.* **63**(7), 1006–1015 (2005)
- R. Winter, J. Moe, and J. Lonstein, Posterior spinal arthrodesis for congenital scoliosis. An analysis of the cases of two hundred and ninety patients, five to nineteen years old. *J. Bone Jt. Surg.*, (1984)
- Z.-X. Wu et al., Accuracy and safety assessment of pedicle screw placement using the rapid prototyping technique in severe congenital scoliosis. *J. Spinal Disord. Tech.* **24**(7), 444–450 (2011)
- G. Wurm, B. Tomancok, P. Pogady, K. Holl, J. Trenkler, Cerebrovascular stereolithographic biomodeling for aneurysm surgery. Technical note. *J. Neurosurg* **100**(1), 139–145 (2004)
- W.-H. Xu, J. Liu, M.-L. Li, Z.-Y. Sun, J. Chen, J.-H. Wu, 3D printing of intracranial artery stenosis based on the source images of magnetic resonance angiograph. *Ann. Transl. Med.* **2**(8), 74 (2014)
- P. Zardini, P. Marino, G. Golia, M. Anselmi, M. Castelli, Ventricular remodeling and infarct expansion. *Am. J. Cardiol.* **72**(19), G98–G106 (Dec. 1993)
- L. Zhou, L. He, H. Shang, G. Liu, J. Zhao, Y. Liu, Correction of hemifacial microsomia with the help of mirror imaging and a rapid prototyping technique: case report. *Br. J. Oral Maxillofac. Surg.* **47**(6), 486–488 (2009)